



ULTRASOUND CASE OF THE DAY

• Eric D. Sale, MD • Michelle L. Rodgers, MD • Lana G. Glenn, R.D.M.S. • Teresita L. Angtuaco, MD •
Department of Radiology, University of Arkansas for Medical Sciences, Little Rock, Arkansas

History

CASE 1

60-year-old woman with a several month history of vague abdominal pain, weight loss, and abnormal liver function tests.

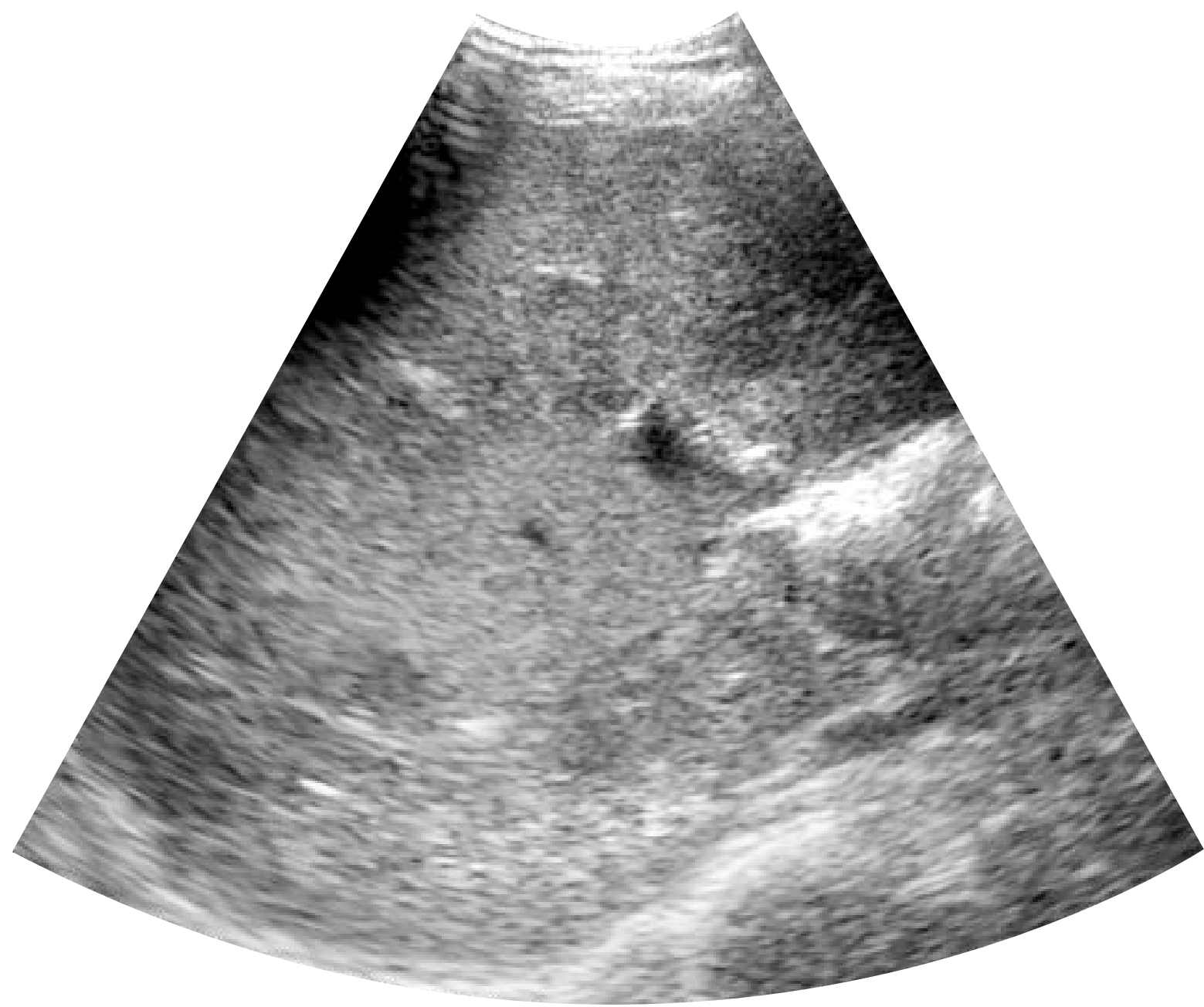


Figure 1a. Transverse abdominal ultrasound, right upper quadrant.



Figure 1b. Transverse abdominal ultrasound, midline at xiphoid.



Figure 1c. Transverse abdominal ultrasound, midline 3 cm below xiphoid.

Diagnosis

Pancreatic carcinoma with liver metastases

Findings

The ultrasound reveals a large hypoechoic mass involving the head of the pancreas along with a markedly dilated pancreatic duct (Fig 1c,d). The liver is diffusely echogenic suggesting hepatic parenchymal disease. Additionally, multiple hypoechoic metastases are noted throughout the liver (Fig 1a,e). Echogenic foci with ring down artifact are seen within the left biliary tree consistent with pneumobilia secondary to prior biliary stent placement due to impending common bile duct obstruction (Fig 1b).

CT demonstrates a heterogeneously enhancing mass in the head of the pancreas causing pancreatic ductal dilatation. The pancreatic mass involves the superior mesenteric vein and abuts the superior mesenteric artery. Multiple low density liver metastases are also demonstrated. Air is visualized in the biliary tree secondary to stent placement in the common bile duct (Fig 1f,g,h).

The patient underwent needle biopsy of celiac lymph nodes and a liver lesion, both of which were positive for adenocarcinoma compatible with a pancreatic primary.

Discussion

Carcinoma of the pancreas is the fourth most common cause of death from cancer in the United States. It is one of the most lethal of all malignancies with a 1-year survival rate of only 8% and a 5-year survival rate of less than 2% (1,2). Pancreatic ductal adenocarcinoma is the most common primary pancreatic neoplasm accounting for between 90% and 95% of all pancreatic neoplasms. This cancer occurs primarily in the elderly with a peak incidence in the seventh and eighth decades, and is rare in those under 40 years of age (3).

The majority (60 - 65%) of pancreatic carcinomas arise in the pancreatic head, 20% in the body, 10% in the tail and 5% to 10% are diffuse (3). Tumors that arise in the head of the pancreas tend to present earlier because of associated bile duct obstruction and jaundice. Carcinomas of the body and tail are typically larger and are more likely to present with metastases. Metastatic disease is most common to the liver, followed by regional lymph nodes, peritoneal carcinomatosis, and to lung. Approximately one-fourth of patients have a palpable, nontender gallbladder called Courvoisier's sign. Other common nonspecific symptoms include weight loss and abdominal pain (1).

The most common sonographic finding in pancreatic carcinoma is a poorly defined, homogeneous or heterogeneous hypoechoic mass in the pancreas. A mass in the uncinate process changes the contour from pointed to a rounded appearance. At the time of diagnosis the tumors usually measure more than 2 cm. Secondary findings of carcinoma include biliary and pancreatic ductal dilatation, vascular and extraglandular invasion, and atrophy of the gland proximal to an obstructing mass (4).

While ultrasonography is frequently used as a screening procedure, it is less consistent in demonstrating the entire pancreas and has not been found to be as sensitive in defining the important findings related to pancreatic malignancies including nodal spread or involvement of major vasculature. CT is valuable in staging as well as determination of tumor resectability. Tumor involvement of the fat surrounding the superior mesenteric artery is considered a sign of unresectability (3,5). MRI is useful to evaluate extension of tumor into peripancreatic tissue in addition to detecting small pancreatic cancers in patients who have enlargement of the pancreatic head without clear definition of tumor on CT examination (3).

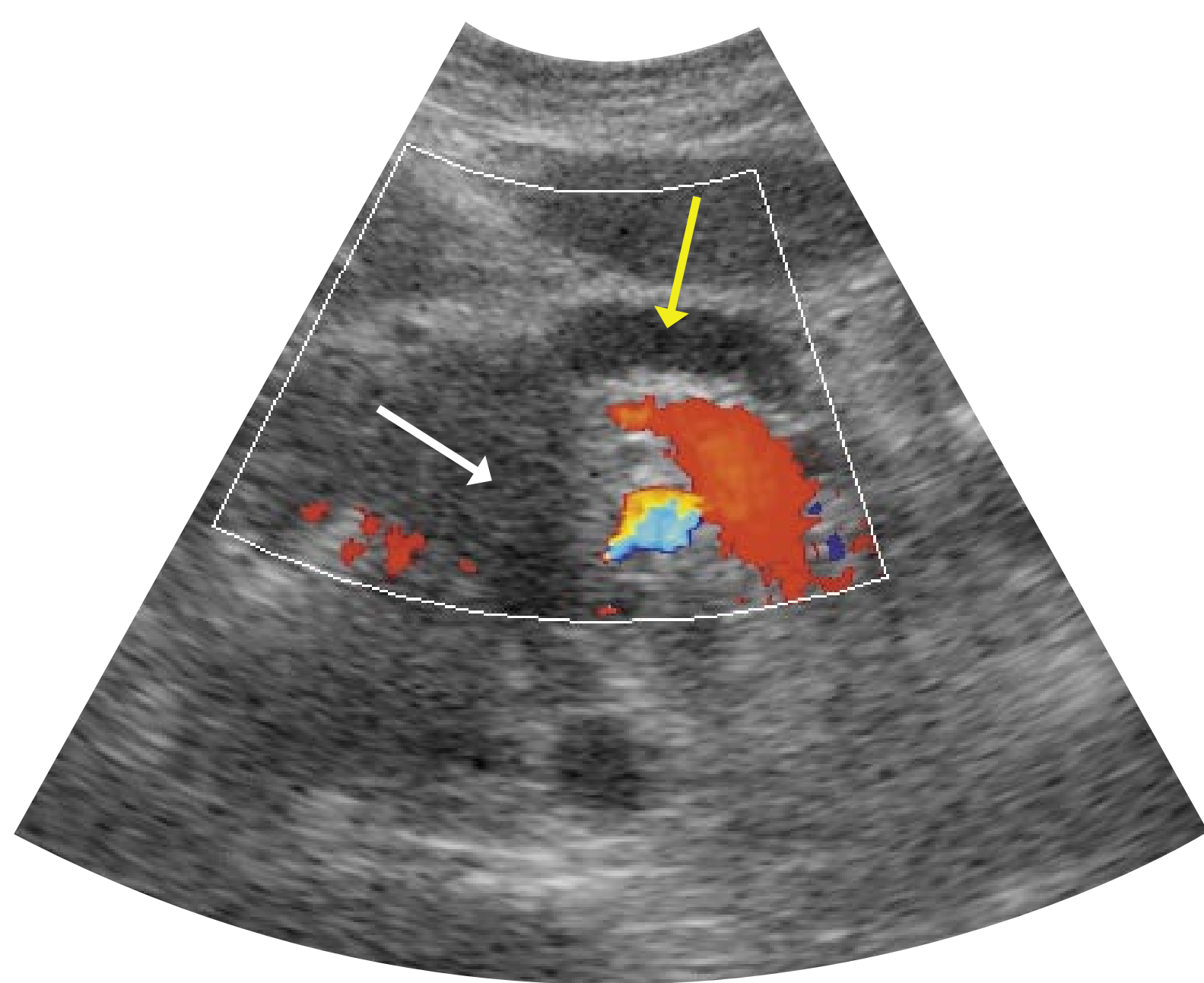


Figure 1d. Transverse ultrasound of the pancreas with color Doppler demonstrates a hypoechoic pancreatic head mass (white arrow) as well as pancreatic ductal dilatation (yellow arrow).

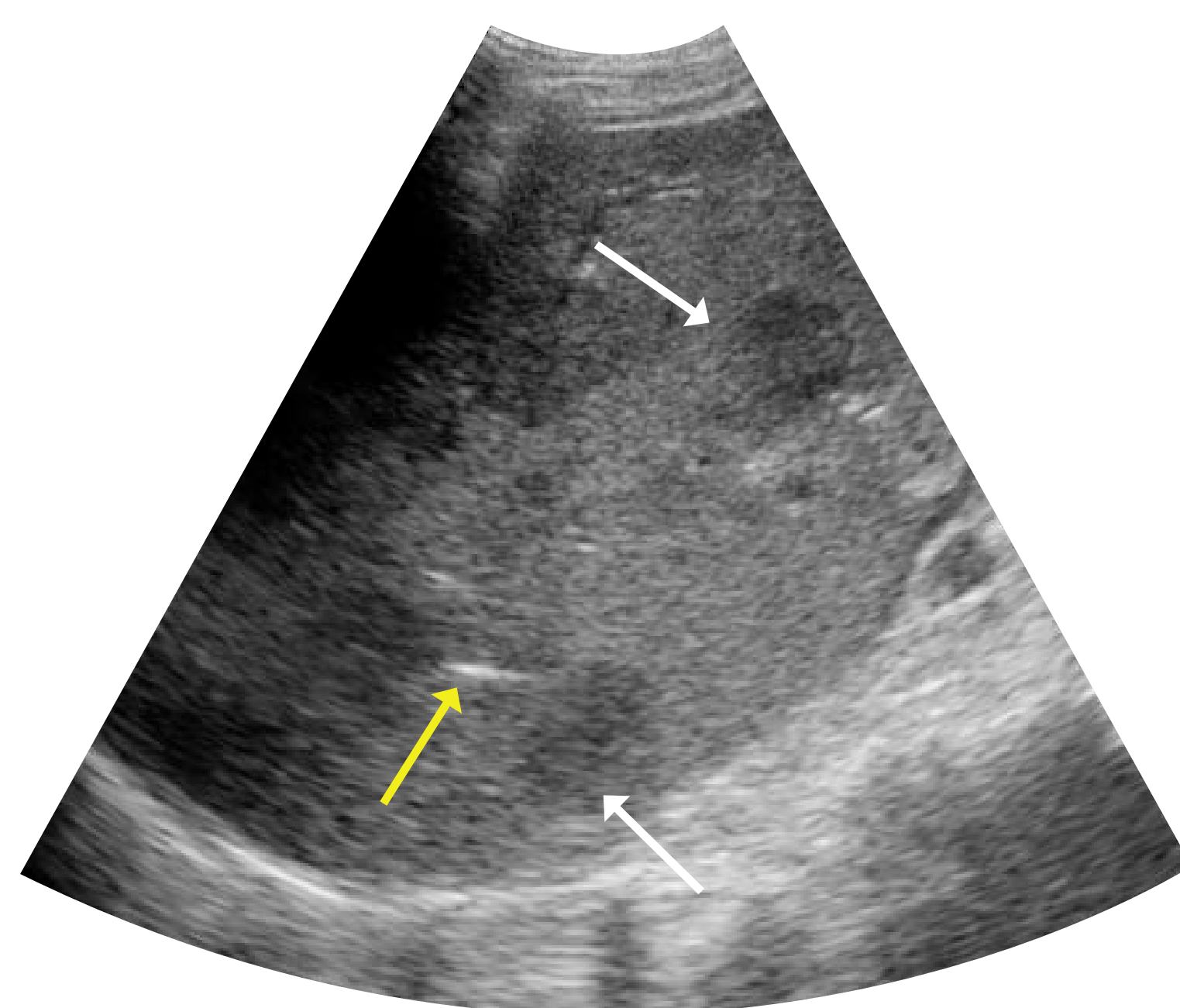


Figure 1e. Longitudinal ultrasound of the liver reveals multiple low density liver metastases (white arrows) as well as pneumobilia (yellow arrow).

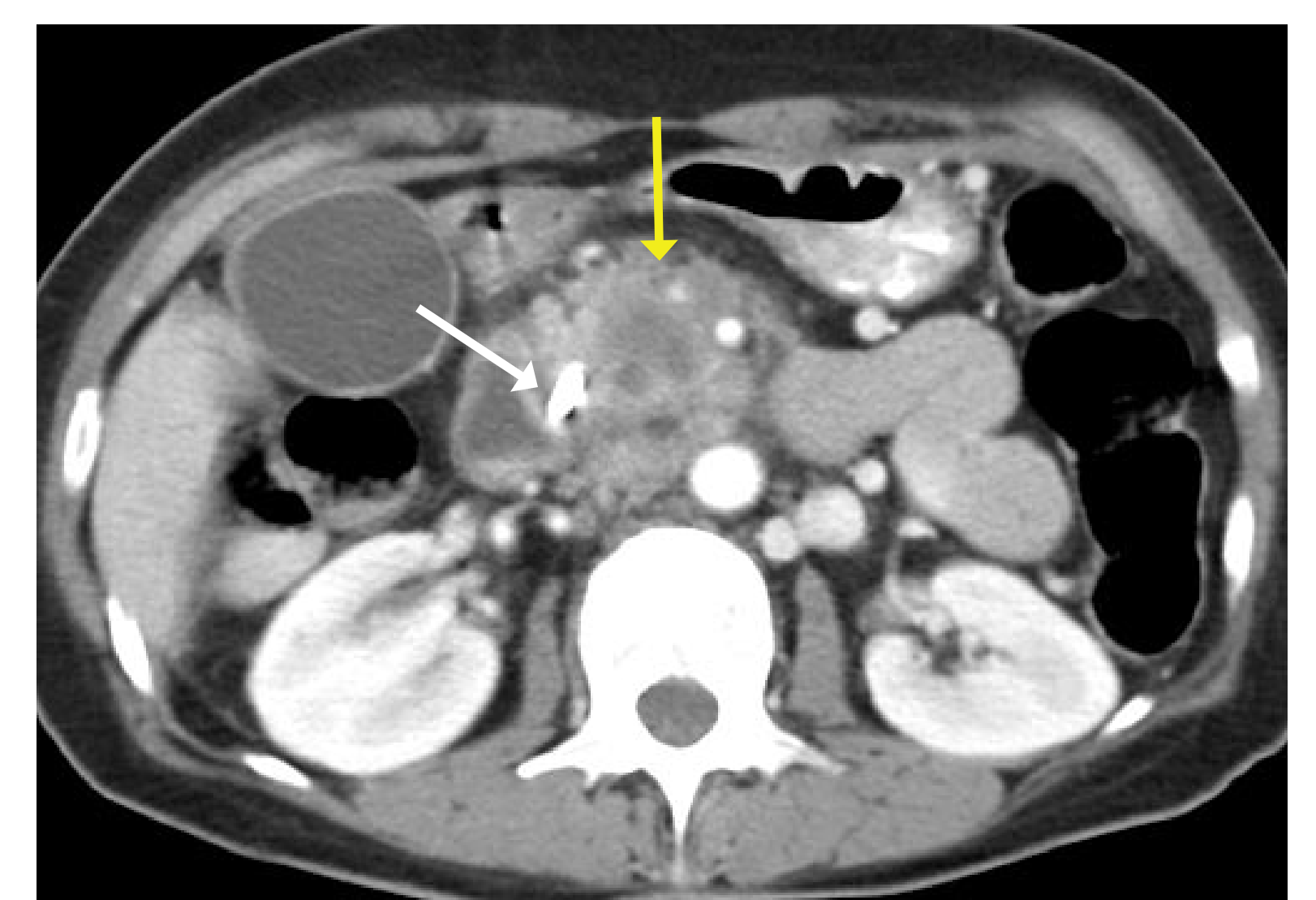


Figure 1f. Axial contrasted CT shows a heterogeneously enhancing pancreatic head mass (yellow arrow). A metallic stent is noted within the distal common bile duct (white arrow).



Figure 1g. Axial CT demonstrates the pancreatic head carcinoma resulting in pancreatic ductal dilatation (arrow).

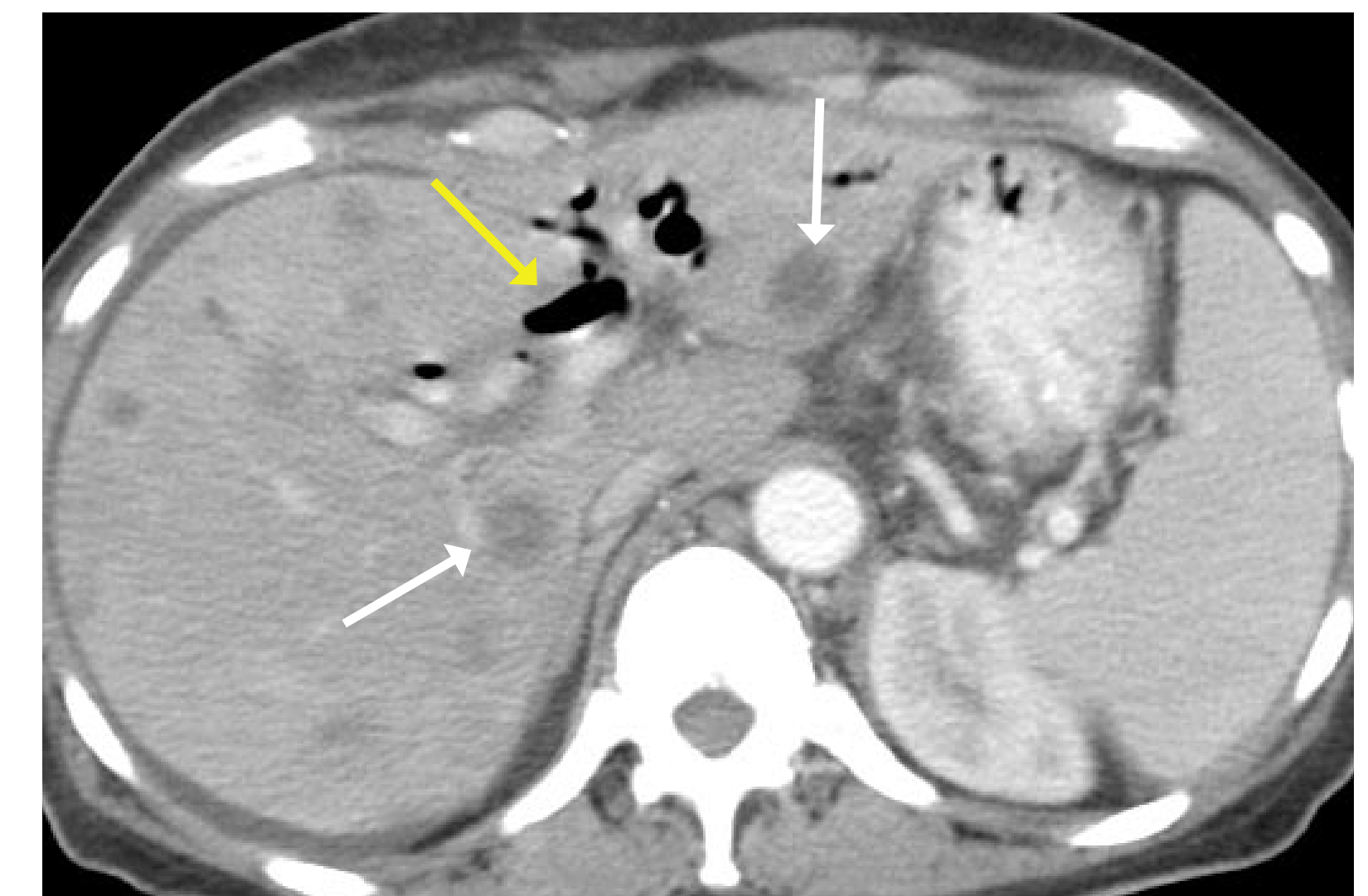


Figure 1h. Axial CT shows multiple liver metastases (white arrows) as well as pneumobilia (yellow arrow).

References

1. Rumack CM, Wilson SR, Charboneau JW. The Pancreas. In: Diagnostic Ultrasound. 2nd ed. Vol 1. St. Louis: Mosby-Year Book, Inc., 1998; 256-268.
2. Kawamura DM, et al. Pancreas. In: Diagnostic Medical Sonography. Abdomen and Superficial Structures. 2nd ed. Philadelphia: Lippincott-Raven Publishers, 1997; 241-261.
3. Lee JK, Sagel SS, Stanley RJ, et al. Pancreas. In: Computed Body Tomography with MRI Correlation. 3rd ed. Vol 2. Philadelphia: Lippincott-Raven Publishers, 1998; 881-902.
4. Jeffrey RB, Ralls PW. The Pancreas. In: Sonography of the Abdomen. New York: Raven Press, 1995; 249-267.
5. McGahan JP, Goldberg BB. Pancreas. In: Diagnostic Ultrasound. A Logical Approach. Philadelphia: Lippincott-Raven Publishers, 1998; 767-776.



ULTRASOUND CASE OF THE DAY

• Michelle L. Rodgers, MD • Eric D. Sale, MD • Lana G. Glenn, R.D.M.S. • Teresita L. Angtuaco, MD •
Department of Radiology, University of Arkansas for Medical Sciences, Little Rock, Arkansas

History

CASE 2

A 38 year old African American female with vague abdominal pain and a positive pregnancy test.



Figure 2a. Longitudinal image of the uterus at the cervix



Figure 2b. Longitudinal Image of the uterus at the fundus

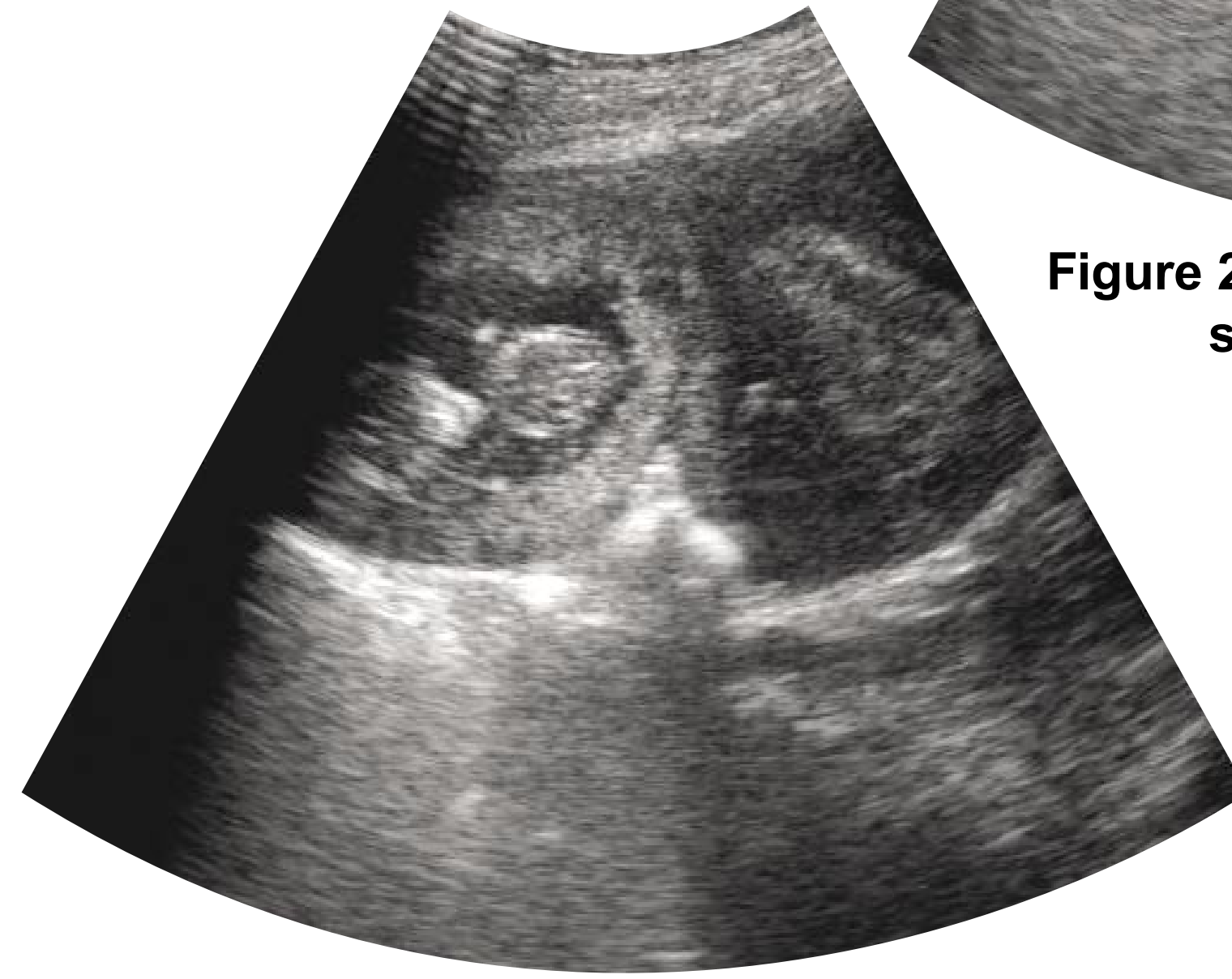


Figure 2c. Transverse image of the right side of the uterine fundus



Figure 2d. Transverse image of the left side of the uterine fundus

Diagnosis

Right tubal ectopic pregnancy with uterine leiomyomata

Findings

Longitudinal images of the uterus show multiple subserosal and transmural myomata (Fig. 2 a and 2b). A gestational sac is seen to the right side of the uterine fundus with an intact embryo (Fig. 2c). The fundus of the uterus is markedly distorted by several leiomyomata (Fig 2d). However, the endometrial canal is seen distinct from the leiomyomata (arrow). A more centered image of the uterine fundus shows the relationship between the intact endometrium (arrow) and the ectopic gestation (Fig. 2e). A 12 week live fetus is seen within the intact gestational sac (Fig 2f and 2g). Because of the patient's past history of infertility and relatively asymptomatic state, the referring obstetrician requested a confirmatory examination. MRI of the pelvis was performed. This confirmed the diagnosis of a right ectopic pregnancy (Fig 2h and 2i). At surgery, the right fallopian tube contained a fetus weighing 27 grams. Several years after the surgery, the patient underwent infertility work-up including a hysterosalpingogram. This showed post salpingectomy changes on the right and obstruction of the left fallopian tube by the uterine leiomyomata. (Fig j)

Discussion

The key in making the diagnosis is the recognition of an empty endometrial cavity. With severe distortion from the uterine leiomyomata, this may be a difficult task. However, once the endometrial echo is recognized, it becomes easy to determine the adnexal location of the gestational sac.

The incidence of ectopic pregnancy in the United States continues to rise; reaching 19.7 per 1,000 as compared to 4.5 per 1,000 just three decades previous. (1) While death from ectopic pregnancies is declining, it is still the most common cause of first trimester maternal death in 90% of cases. Numerous risk factors have been reported for ectopics and include: prior pelvic inflammatory disease, prior tubal sterilization with reversal, treatment for infertility, prior ectopics, diethylstilbestrol exposure, IUD use, and lifestyle (1). The current litera-

ture reports the presence of leiomyomata impairs fertility in an estimated 10 % of cases. Intracavitary leiomyoma have been shown to have deleterious effect on embryo implantation. Perhaps this impact on fertility causes these women to seek fertility assistance, thus raising their risk of ectopic pregnancy (2).

Leiomyomata are common in reproductive age women(3) and is the leading cause of hysterectomy in America (4). The effect of these tumors on reproductivity is more difficult to define given their prevalence and is the subject of much scrutiny. Many hypotheses attempt to explain or identify a causal relationship between leiomyomata and decreased fertility. Some believe the presence of leiomyomata have a deleterious effect on sperm transport, implantation, uterine perfusion and contractility (3). Additional hypotheses raise the possibility of mechanical distortion of the endometrial cavity by submucosal fibroids as cause for poor implantation. Some believe that the presence of leiomyomata creates inflammatory and vascular changes with abnormal release of growth factors deleterious in implantation and pregnancy(3). Infertile patients may choose to undergo myomectomy in hopes of improving their chances of conceiving (3).

It is recognized that leiomyomata are associated with maternal abdominal discomfort, intrauterine growth restriction, intrauterine fetal demise, preterm labor, abruptio placentae, and dystocia at birth (5). Contrary to popular opinion, fibroids neither shrink nor grow during pregnancy (4) despite their hormonal sensitivity. Recent hypotheses suggest that parity may be protective against fibroids with an inverse relationship between risk of fibroids and increasing parity. Researchers hypothesize that the effects of postpartum uterine involution (apoptosis, proliferation and ultimately, remodeling), can result in the loss of leiomyomata (4).

When clinical concerns warrant a confirmatory test, MRI remains the best examination of choice because it shows a clear delineation of the endometrial echo relative to the uterine leiomyomata and the adnexa. Red or hemorrhagic degeneration of leiomyomata are also well demonstrated by T2 and T1 weighted MRI images (6). This massive hemorrhagic infarction of the myoma is usually accompanied by severe pain. Although the long term effect of MRI on fetuses is unknown, this is an alternative when ultrasound fails to elucidate a cause for the patient's clinical condition. In this case, the right tubal gestation is documented to be intact and located clearly to the right of the uterine fundus.

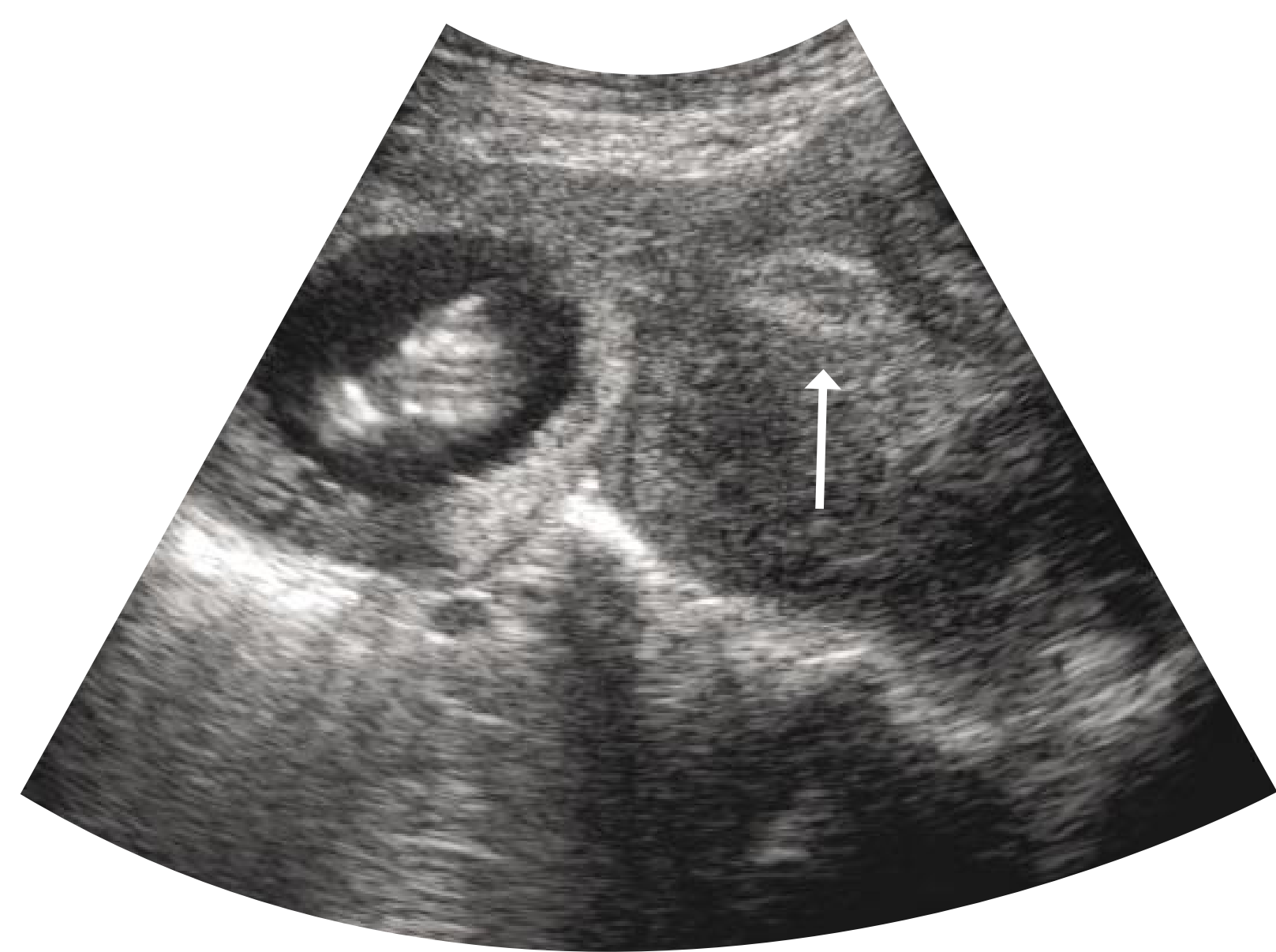


Figure 2e. Transverse view of the uterine fundus at midline

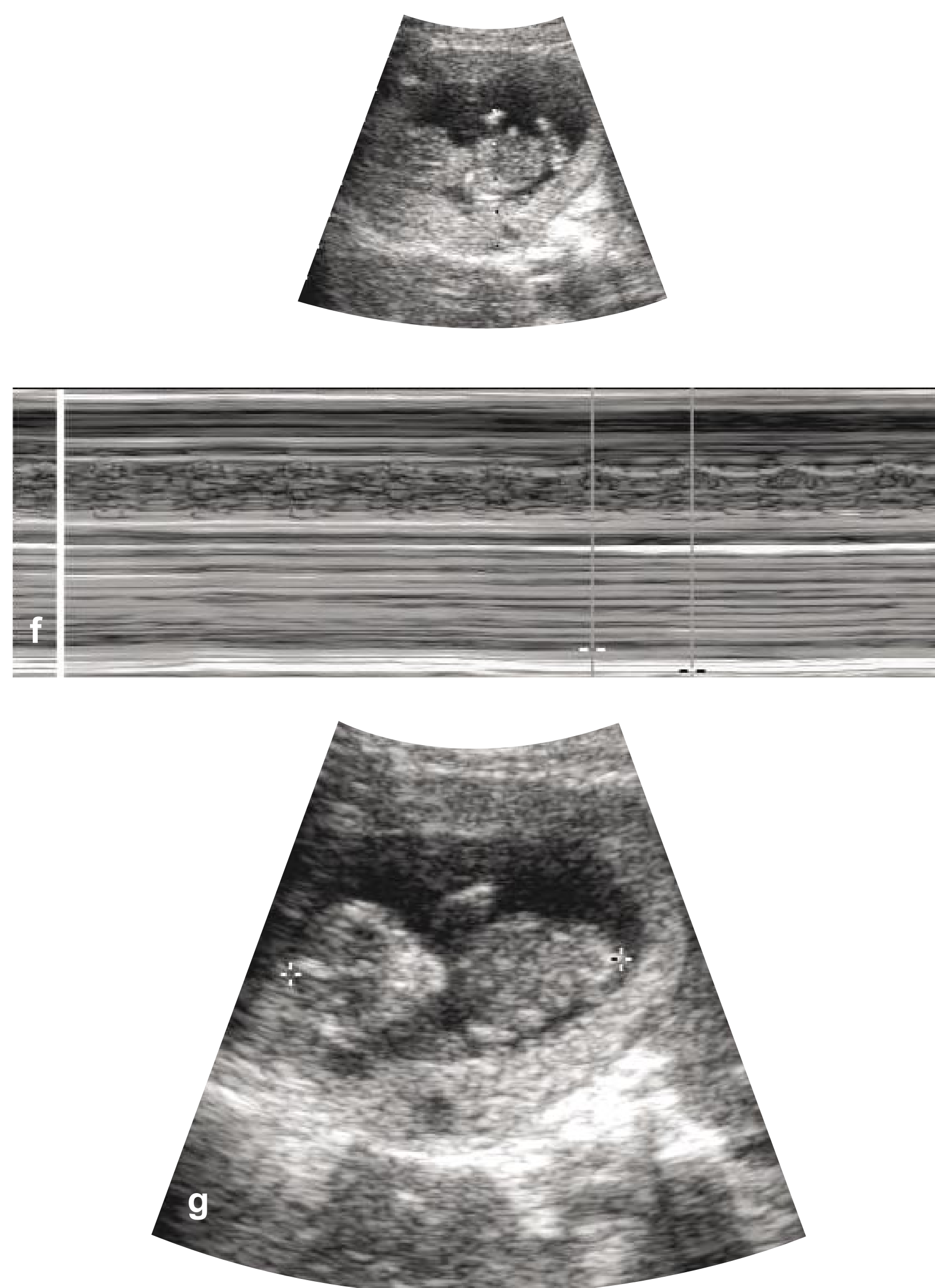


Figure 2f and 2g. Intact fetal pole with cardiac pulsations in the right adnexa

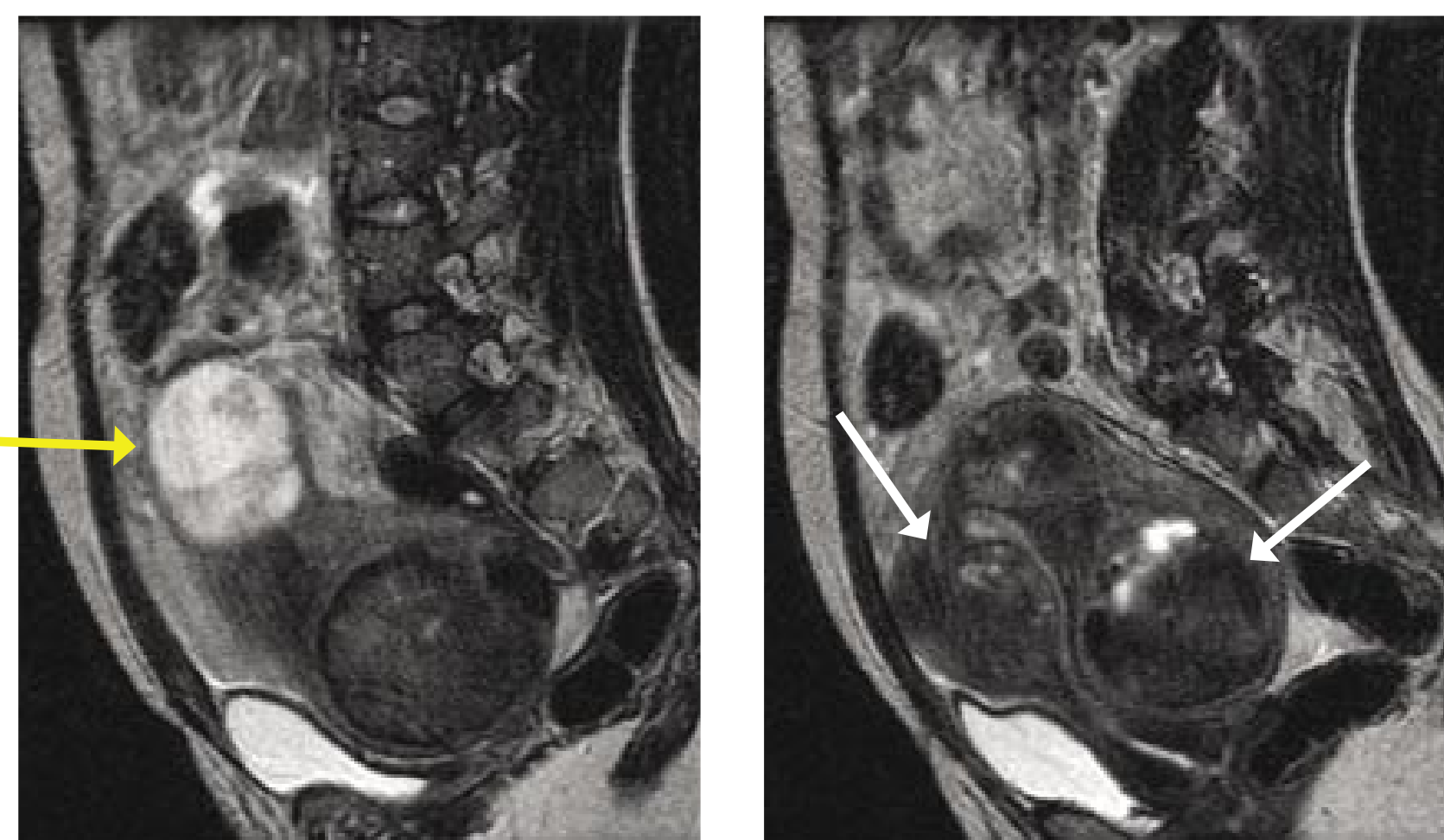


Figure 2h and 2i. T2-weighted sagittal MRI images to the right of midline and at midline confirm the ectopic gestation (yellow arrow) to the right of the uterine fundus and multiple degenerating leiomyomata (white arrow)

Figure 2j. Hysterosalpingography showing post-salpingectomy changes on the right and left tubal obstruction.



References

1. Pisarska, Margareta D. MD; Carson, Sandra A. MD. Incidence and risk factors for ectopic pregnancy. CLIN OBSTET GYNECOL 1999; 42 (1):2-8.
2. Hart, Roger. Unexplained infertility, endometriosis, and fibroids. BRIT MED J 2003; 327(7417): 721-724.
3. Surrey, Eric S. MD; Lietz, Annette K. LPN.; Schoolcraft, William B. MD. Impact of intramural leiomyomata in patients with a normal endometrial cavity on in vitro fertilization-embryo transfer cycle outcome. FERTIL STERIL 2001; 75(2): 405-410.
4. Day Baird, Donna, Dunson, David B. Why is parity protective for uterine fibroids? EPIDEMIOLOGY 2003; 14 (2): 247-250.
5. Courban, Daniella MD.; Blank, Stephanie MD.; et al. Acute renal failure in the first trimester resulting from uterine leiomyomas. AM J OBSTET GYNECOL 1997; 177(2): 472-473.
6. Nishino, Mizuki; Hayakawa, Katsumi; Iwasaku, Kazuhiro; Takasu, Kosho. Magnetic resonance imaging in gynecological emergencies. J COMPUT ASSIST TOMOGR 2003; 27(4): 564-570.



ULTRASOUND CASE OF THE DAY

• Michelle L. Rodgers, MD • Eric D. Sale, MD • Lana G. Glenn, R.D.M.S. • Teresita L. Angtuaco, MD •
Department of Radiology, University of Arkansas for Medical Sciences, Little Rock, Arkansas

History

A 33 year old African American female, G4P1A2, presented to the Emergency Department with acute onset of lower abdominal pain and spotting. Initial testing in the Emergency Department revealed a positive urine pregnancy test. The patient was referred to Radiology for an ultrasound evaluation.

CASE 3

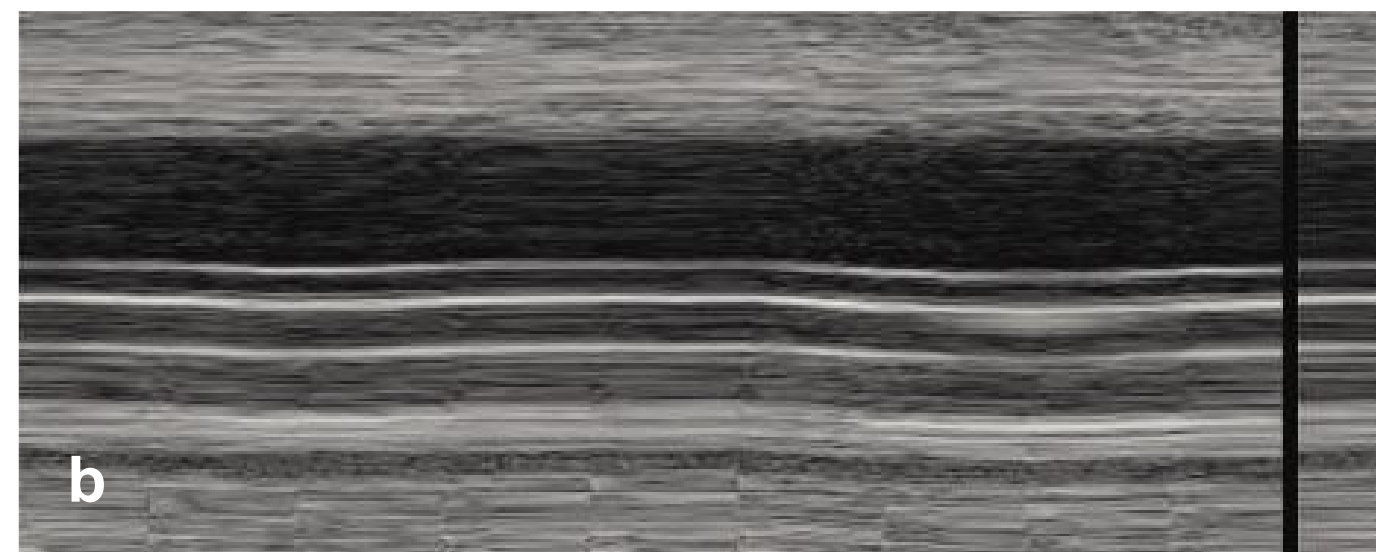
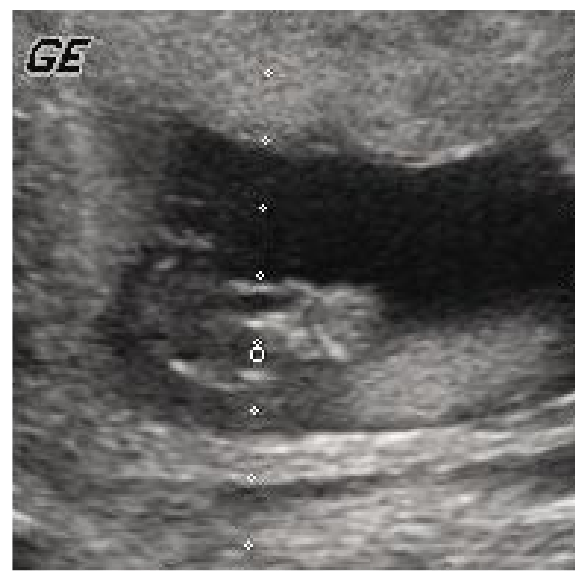


Figure 3a and 3b. Transverse views of the uterus

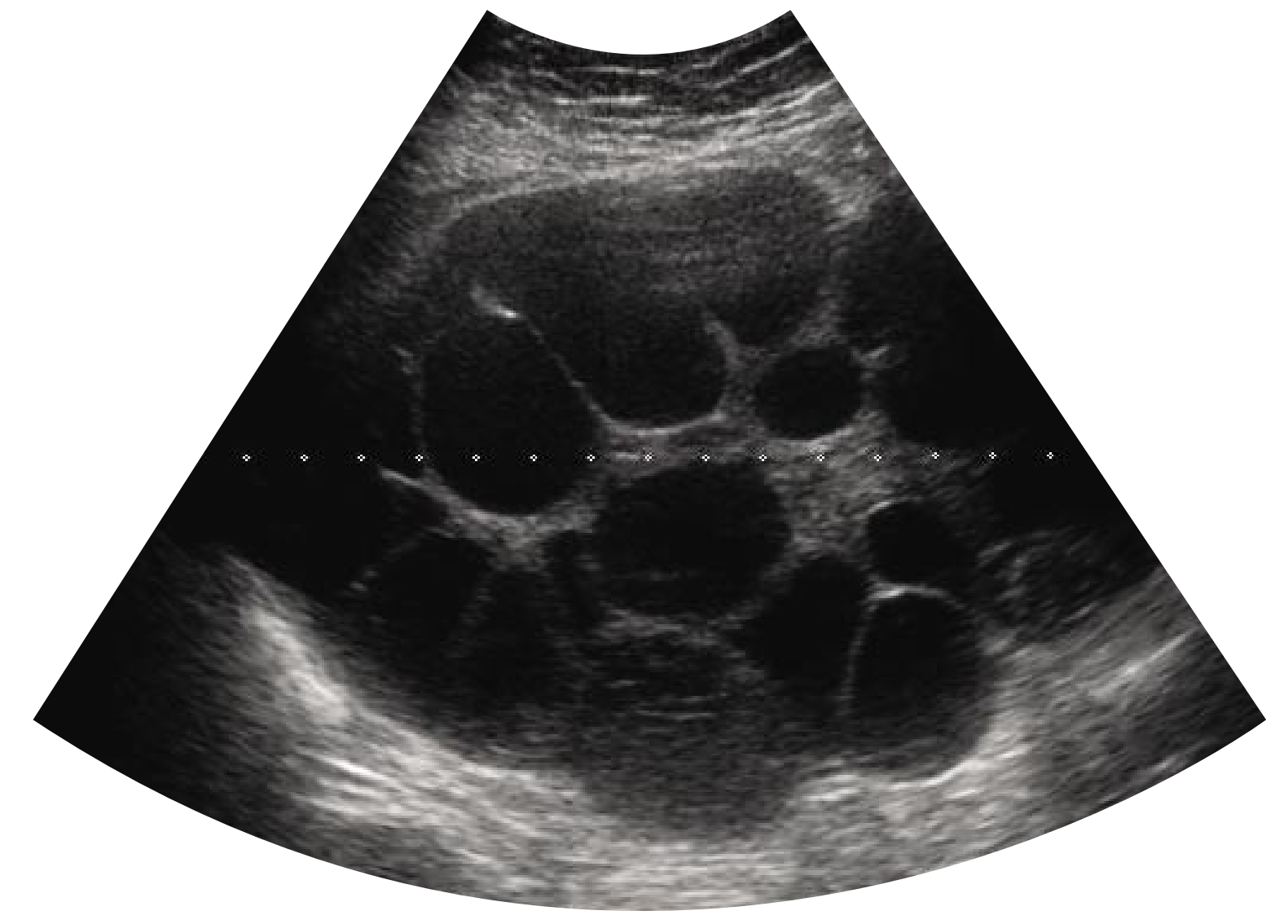


Figure 3c. Transverse view to the right of the uterus



Figure 3d. Transverse view to the left of the uterus

Diagnosis

Hyperreactio luteinalis

Findings

Transabdominal scanning identified a single intrauterine pregnancy measuring approximately 10 weeks. No cardiac activity was detected (Fig. 3a and b). The right ovary measured 17.8cm by 13 cm (Fig 3c) and the left 12.4 cm by 8.0 cm (Fig 3d). Both ovaries contained multiple large cysts. The patient proceeded to spontaneously abort but persisted to have vaginal spotting. A repeat ultrasound examination was done eight weeks from the initial study. The ovarian cysts have resolved (Fig 1e and f). The endometrial cavity however was filled with hypervascular tissue which appeared to penetrate the myometrium (Fig 3 g and 3 h). Suspicion for molar tissue was raised and dilation and curettage was performed. Pathology revealed tissue consistent with retained products of conception.

Discussion

Hyperreactio luteinalis is a rare complication of pregnancy clinically similar to iatrogenically induced ovarian hyperstimulation syndrome (1). Overproduction of ovarian stromal androgens by theca lutein cells results from increased sensitivity to human chorionic gonadotropin levels (1). This results in moderate to severe cystic ovarian changes occurring in response to elevated circulating gonadotrophins associated with pregnancy (2). Patients may present with ascites, pleural effusions, virilization, and markedly enlarged, painful ovaries (1). Within weeks after delivery or termination of pregnancy, the cysts resolve and the ovaries return to their normal pre-pregnant state.

Controversy remains as to the management of adnexal masses in pregnancy (3). One approach is based on criteria suggesting malignancy versus benignity. Criteria incorporated in one series included size (greater than 4.0 cm), number of septations (greater than three), and character of internal contents (solid versus anechoic) (4). In this particular series, the lesions measuring less than 4 cm. turned out to be benign.

However, lesions containing multiple or thick septations were less likely to be benign as were lesions containing echogenic debris. These criteria are also employed in non-gravid patients. Some have advocated removal of any mass >6 cm that persists into the second trimester unless the mass is felt to represent a leiomyoma (5). In a series of 7,996 second and third trimester patients, 4.1% demonstrated ultrasonographically detectable adnexal masses (4). Most masses are corpus luteum cysts most of which resolve spontaneously by 16 weeks gestation (3). In the case of hyperreactio luteinalis cysts, most resolve within weeks of parturition or termination/loss of the pregnancy (2) as in the case of this patient.

Given improvements in modern technology and ultrasonography, more adnexal masses may be discovered in pregnancy than ever before. In patients presenting with symptoms of ovarian hyperstimulation syndrome without a history of pharmacologic fertility treatments, a diagnosis of hyperreactio luteinalis should be entertained to avoid unnecessary surgical intervention (1).

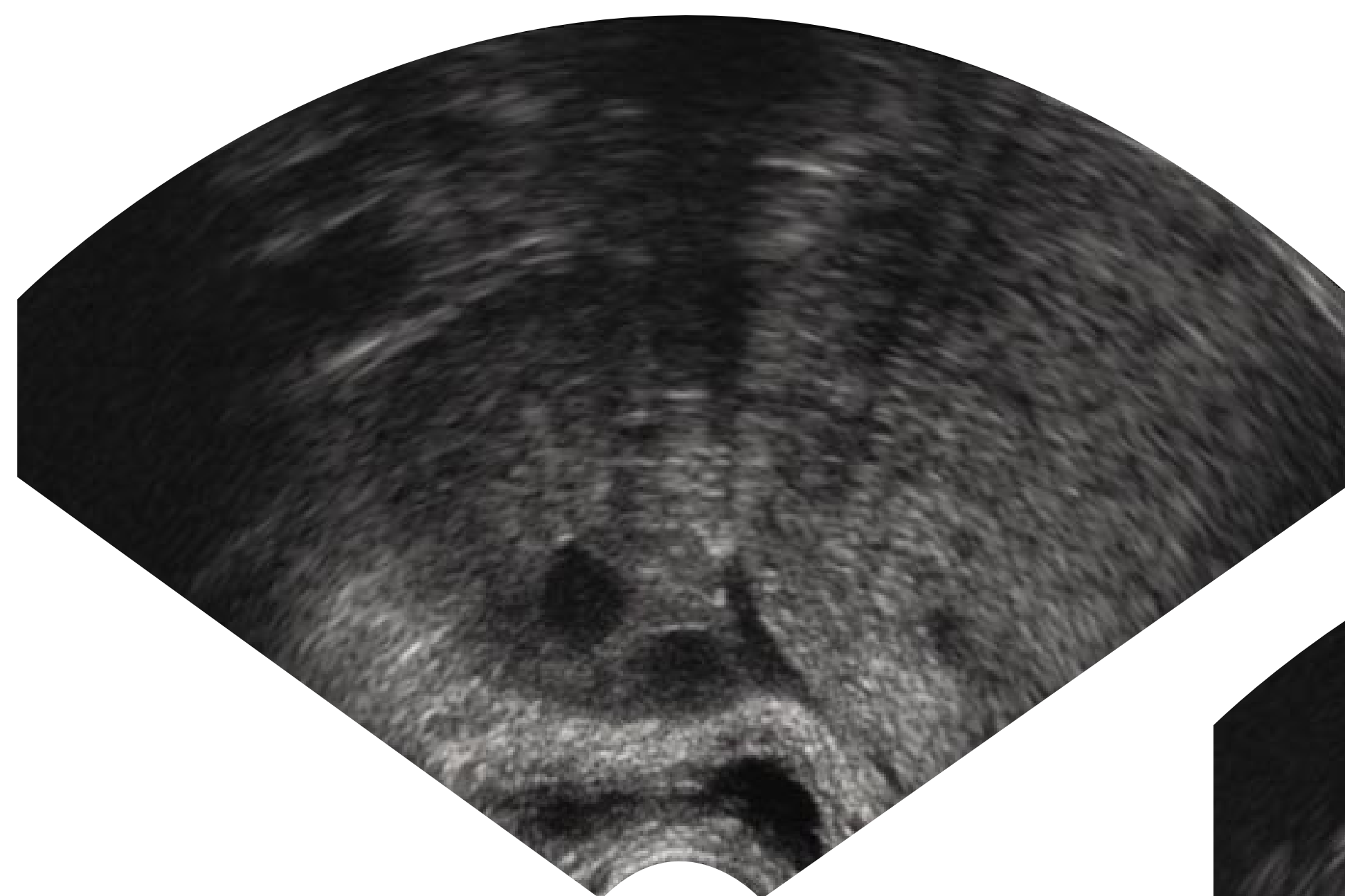


Figure 3e. Endovaginal image of the right ovary

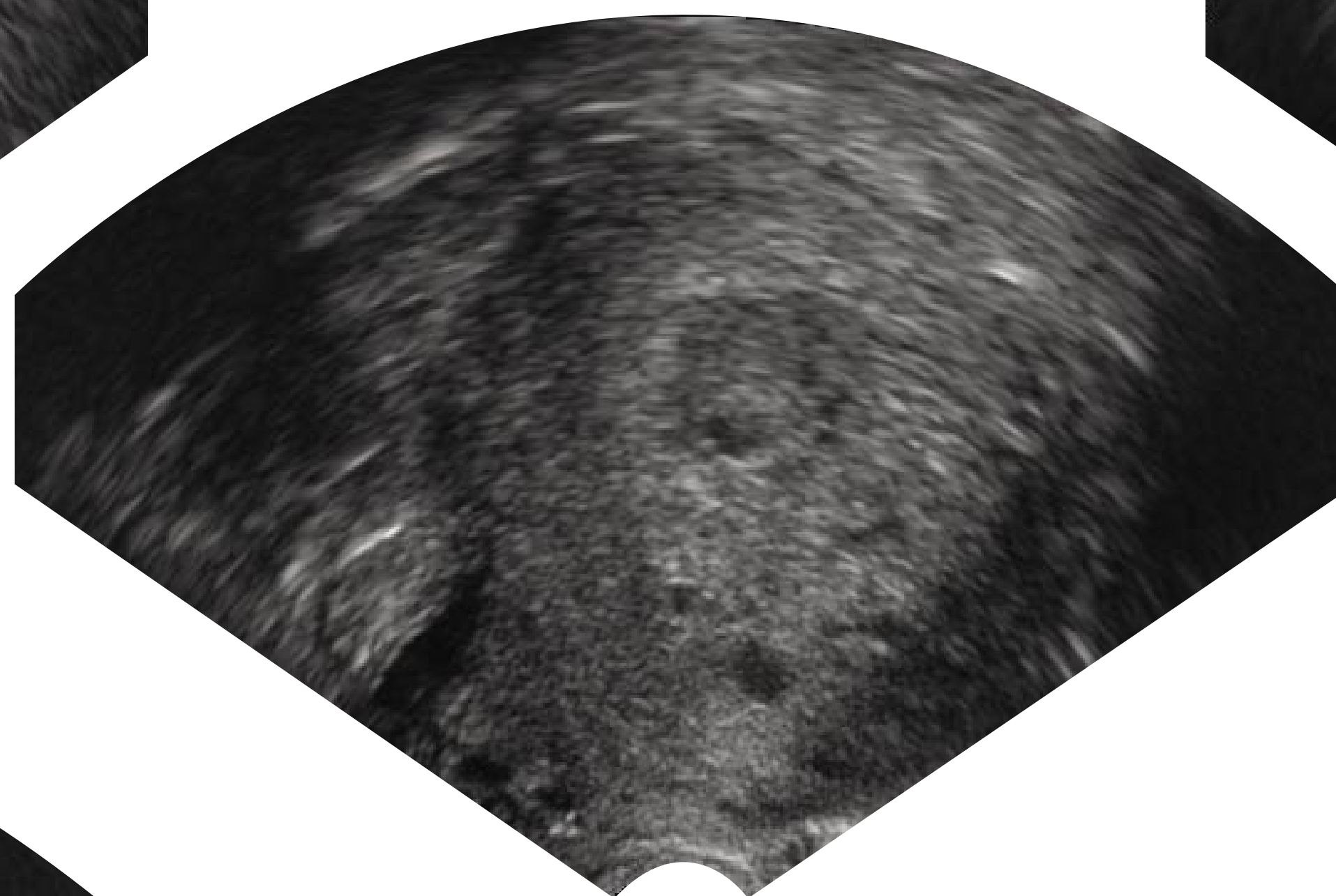


Figure 3g. Sagittal endovaginal image of the uterus

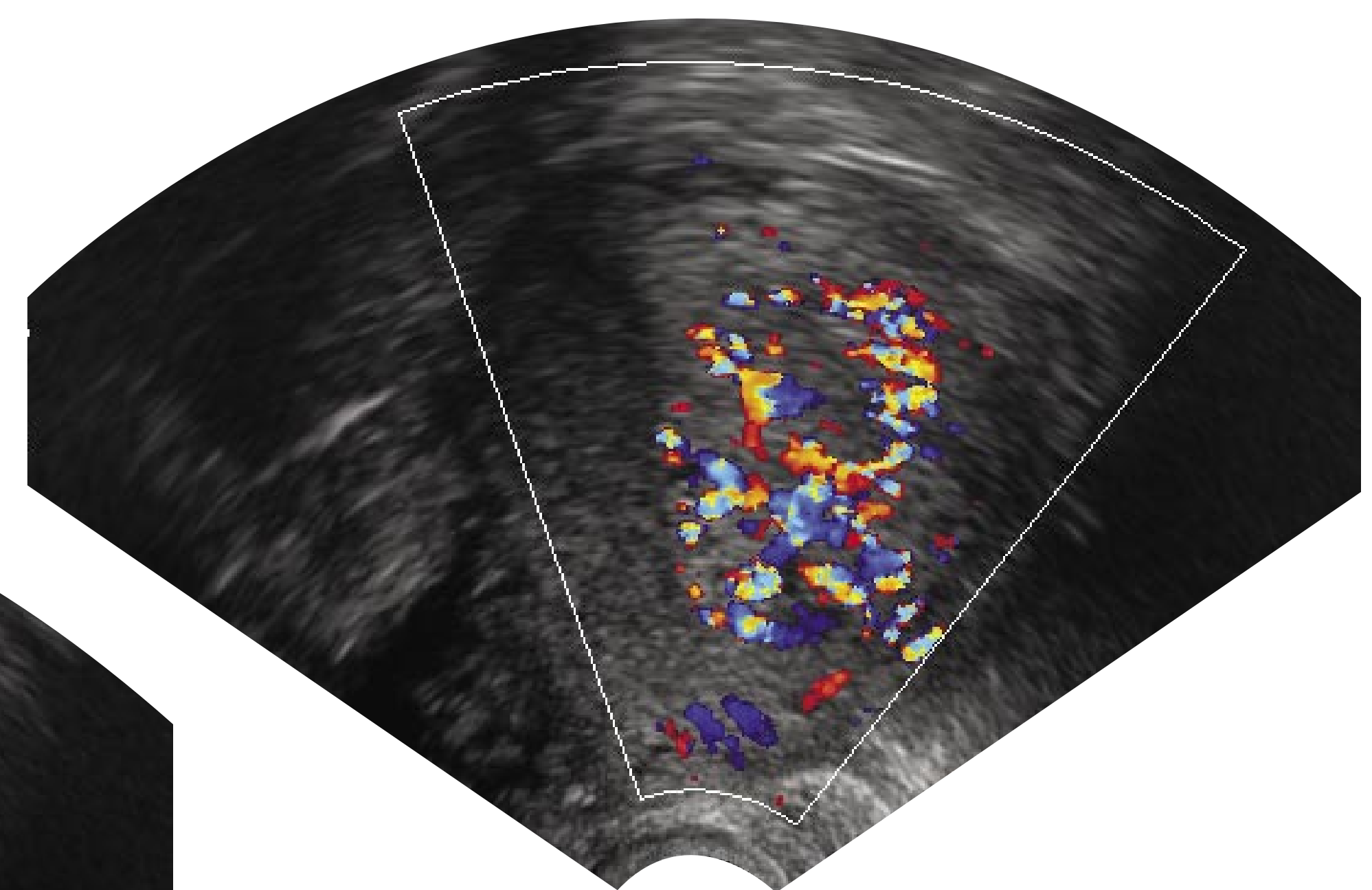


Figure 3h. Sagittal Color Doppler image of the uterus

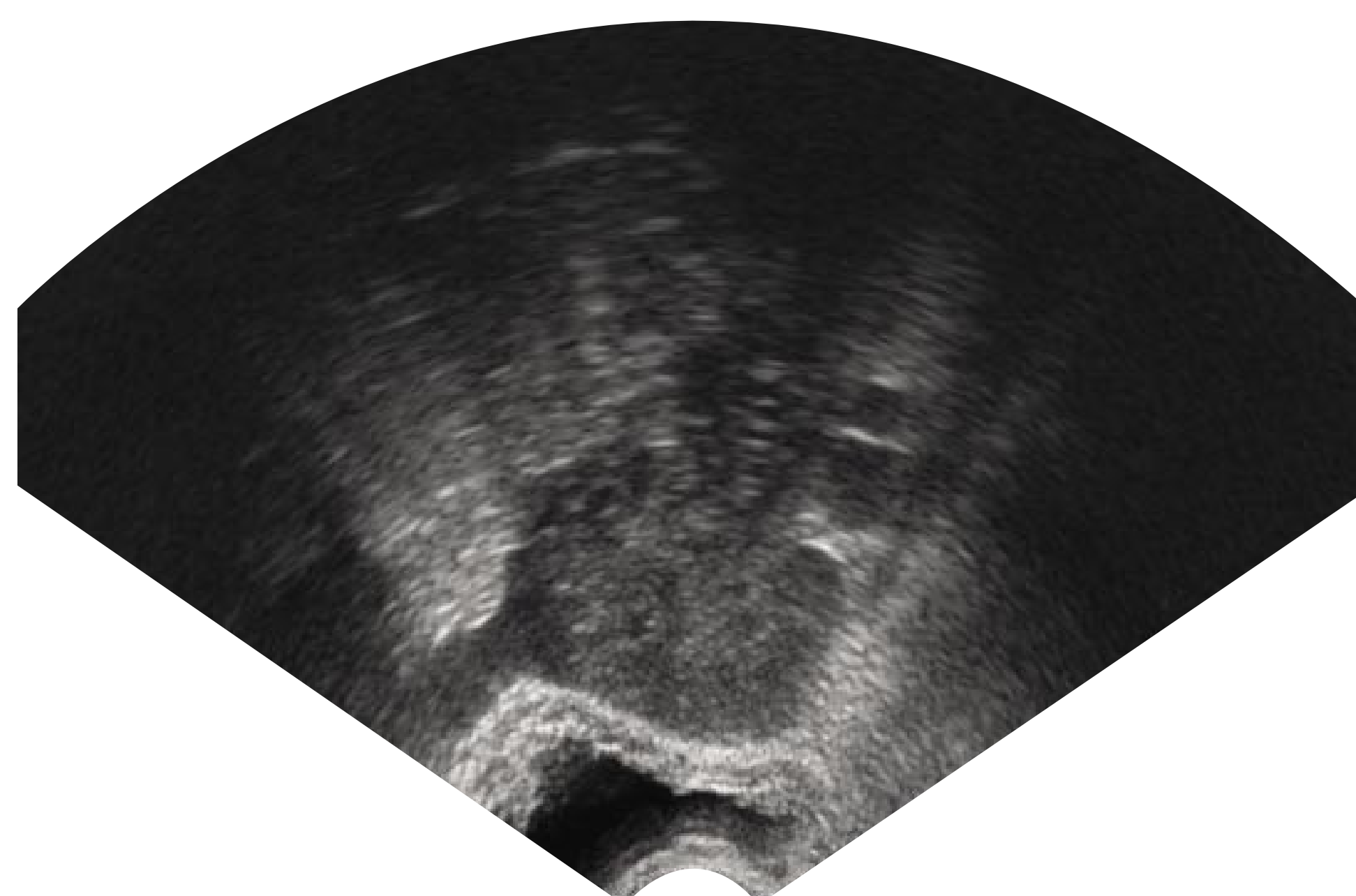


Figure 3f. Endovaginal image of the left ovary

References

1. Foulk, Russell A. MD; Martin, Mary C. MD; Jerkins, Gregory L. MD; Laros, Russell K. MD. Hyperreactio luteinalis differentiated from severe ovarian hyperstimulation syndrome in a spontaneously conceived pregnancy. *AM J OBSTET GYNECOL* 1997; 176: 1300-1302.
2. Akkus, Emre; Carrier, Serge, et al. Duplex ultrasonography after prostaglandin E1 injection of the clitoris in a case of hyperreactio luteinalis. *J UROL* 1995; 153: 1237-1238.
3. Platek, Deborah N. MD; Henderson, Cassandra E. MD; Goldberg, Gary L. MD. The management of a persistent adnexal mass in pregnancy. *AM J OBSTET GYNECOL* 1995; 173 (4): 1236-1240.
4. Hill, Lyndon M. MD; Connors-Beatty, D.J. MA; Nowak, Anita RDMS; Tush, Brenda RDMS. The role of ultrasonography in the detection and management of adnexal masses during the second and third trimesters of pregnancy. *AM J OBSTET GYNECOL* 1998; 179 (3): 703-707.
5. Akira, Shigeo MD; Yamanaka, Atsuko MD et al. Gasless laparoscopic ovarian cystectomy during pregnancy: comparison with laparotomy. *AM J OBSTET GYNECOL* 1999; 180 (3): 554-557.



ULTRASOUND CASE OF THE DAY

• Michelle L. Rodgers, MD • Eric D. Sale, MD • Lana G. Glenn, R.D.M.S. • Teresita L. Angtuaco, MD •
Department of Radiology, University of Arkansas for Medical Sciences, Little Rock, Arkansas

History

CASE 4

A 17 year old female presented at 22 weeks gestation with a vaginal mass which the patient noted was increasing in size. The ultrasound demonstrated a normal single intrauterine pregnancy. Multiple transabdominal and endovaginal images of the mass were obtained.

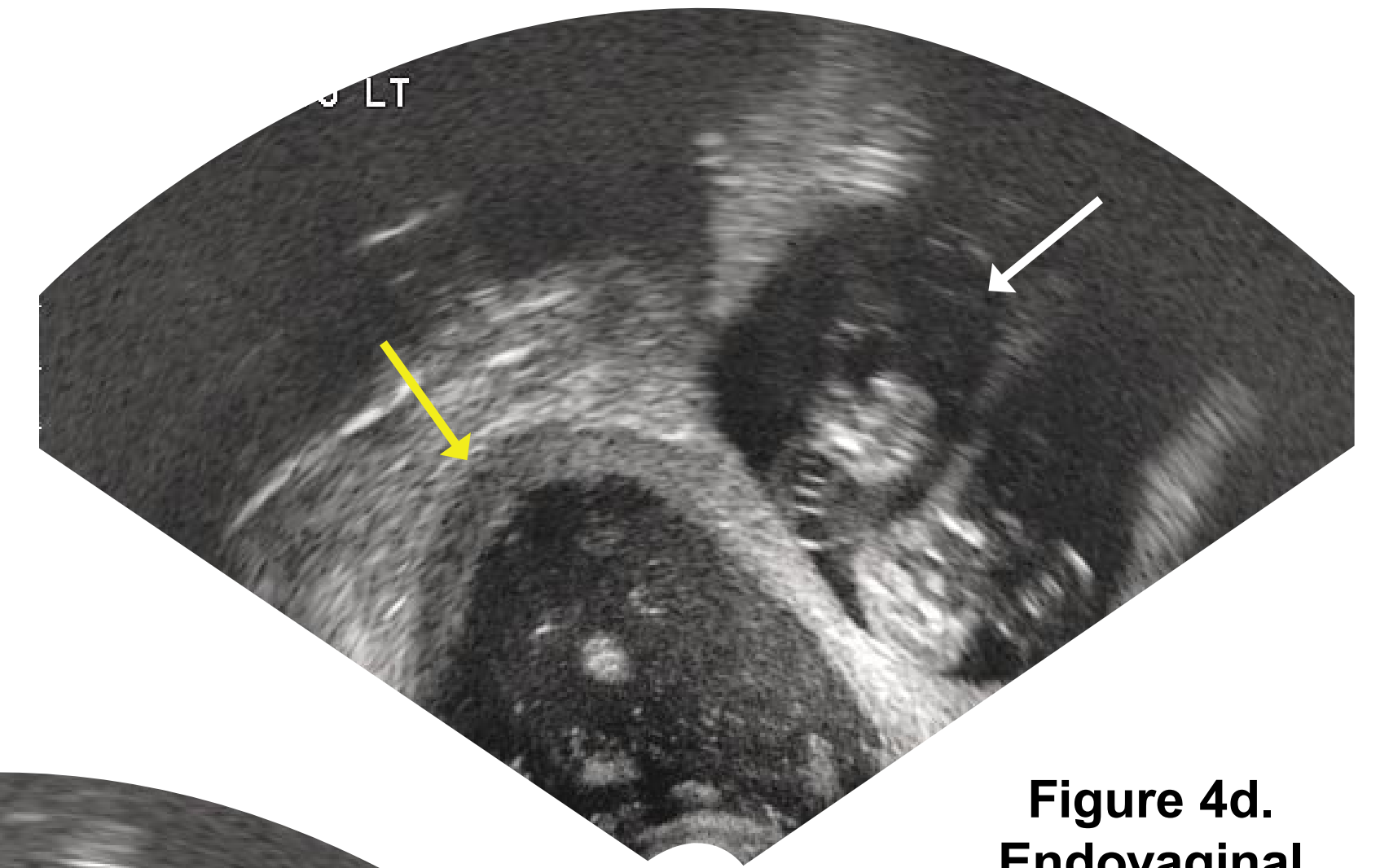
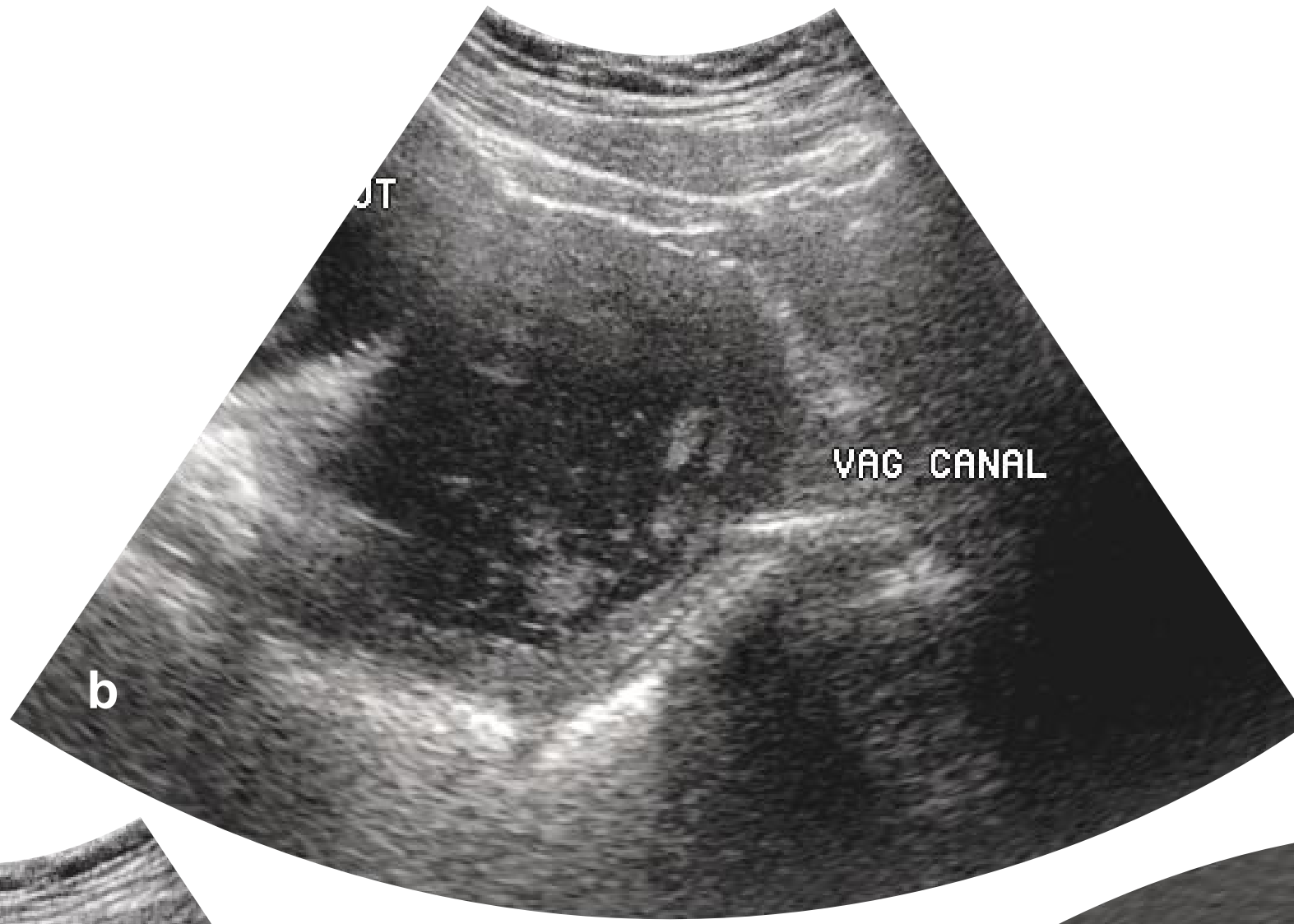
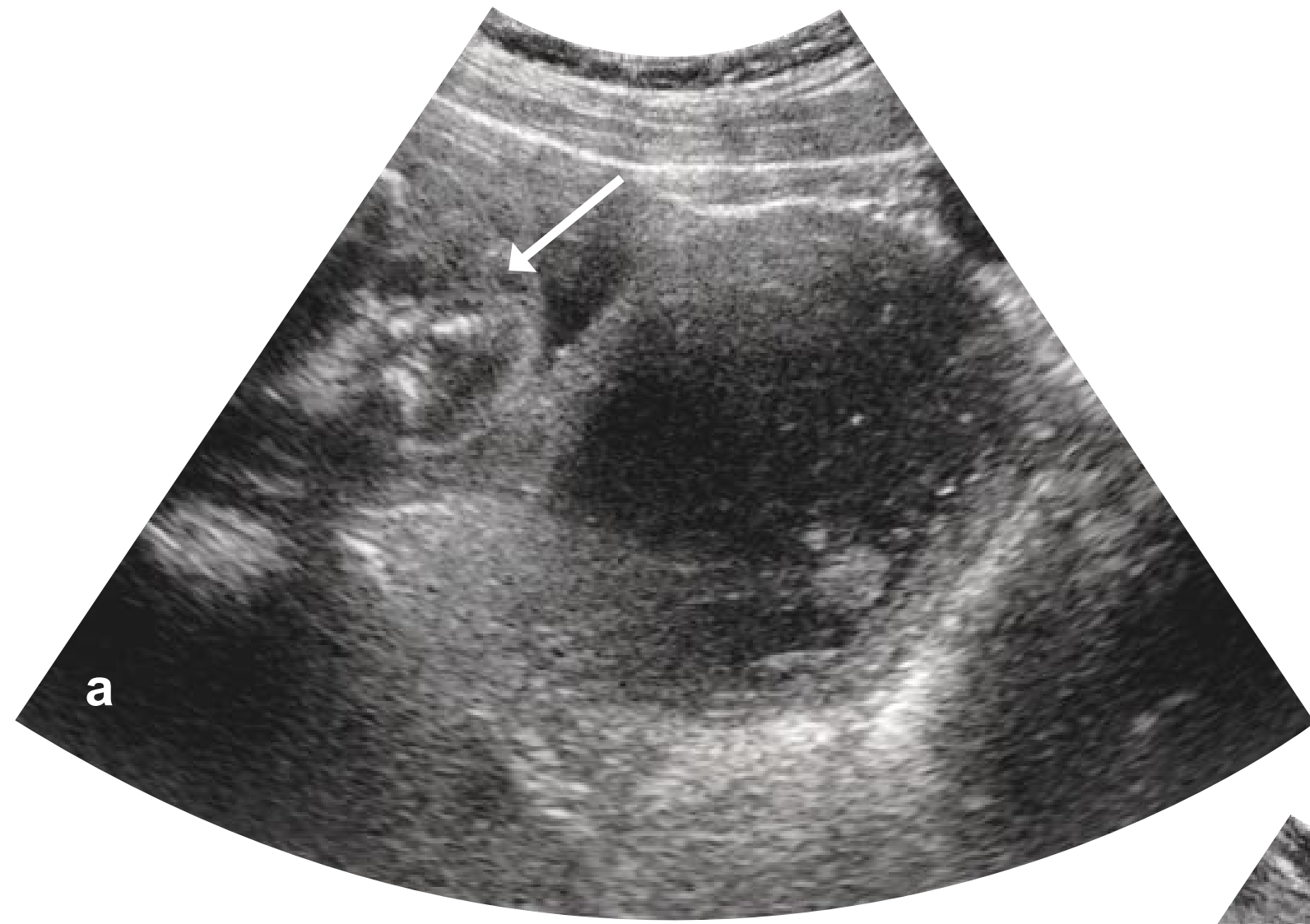


Figure 4a-4c. Longitudinal images at the level of the cervix showing the mass and its relationship to the normal fetus and the vaginal canal.



Figure 4d. Endovaginal sagittal view of the mass (yellow arrow) and its relationship to the presenting fetal parts (white arrow)

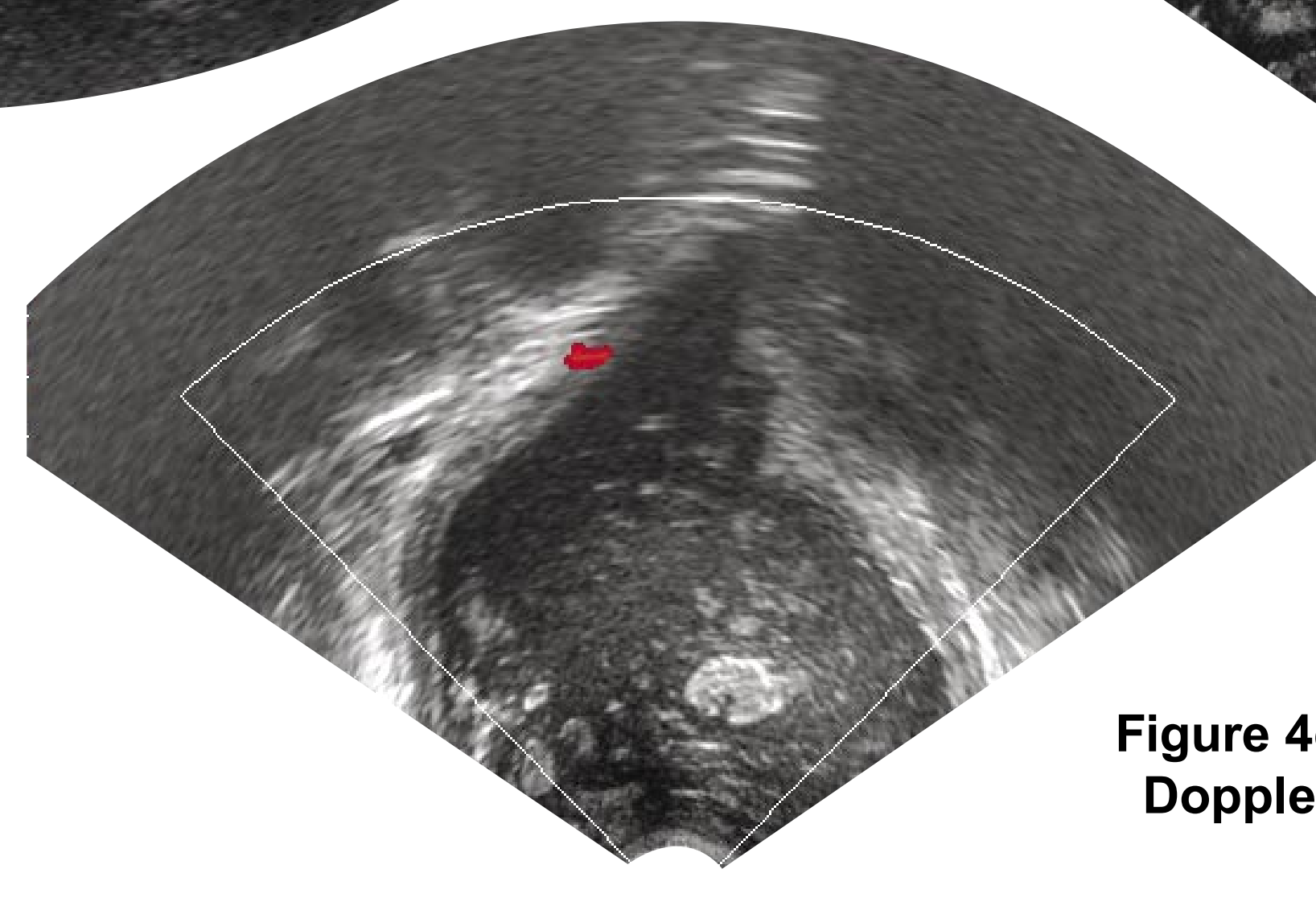


Figure 4e. Endovaginal color Doppler image of the mass

Diagnosis

Uterus Didelphys with single intrauterine pregnancy in the left uterine cavity and hematometocolpos on the right.

Findings

Transabdominal images show the presenting fetal rump (white arrow) just superior to the mass which appears to fill the upper vagina (Fig. 4a and 4b). The mass had floating debris that showed dependent layering and change in position during the examination (Fig. 4c, 4d and 4e). The mass was non-tender and showed no vascularity. There is a rim of myometrium surrounding the mass which is best seen on the endovaginal images. The fetus measured 22 weeks gestation and showed no abnormality. Because of the location of the mass, a Cesarean section was planned. MRI was requested to further characterize the mass and determine the course of management. MRI images show a normal intrauterine pregnancy in the left uterine cavity of a uterus didelphys. The mass seen on ultrasound corresponded to the obstructed upper vagina connected to the right uterine cavity. On the coronal images, there were two fluid collections identified, a smaller more superior uterine cavity (yellow arrow) and a larger obstructed upper vagina seen inferiorly (white arrow). At Cesarean section, the obstructing vaginal septum was removed. Both mother and baby did well.

Discussion

Mullerian duct anomalies (MDAs) are reported to occur in 5-6% of women. These MDAs include unicornuate and bicornuate uteri, septate uterus, uterine hypoplasia, uterine agenesis, and uterus didelphys (1). Uterus didelphys has a reported incidence of 1.2%, representing nearly 20% of all MDA (1).

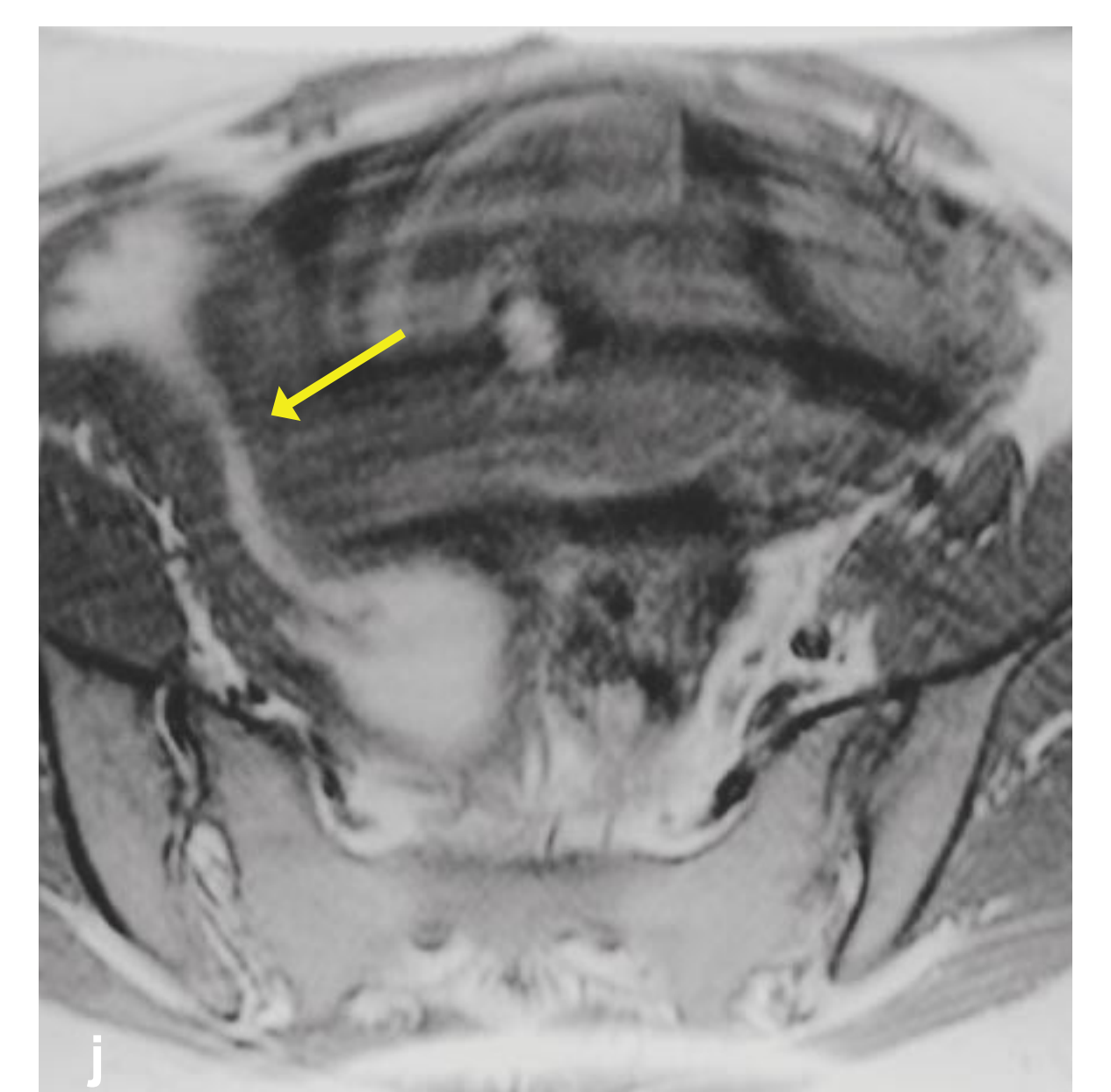
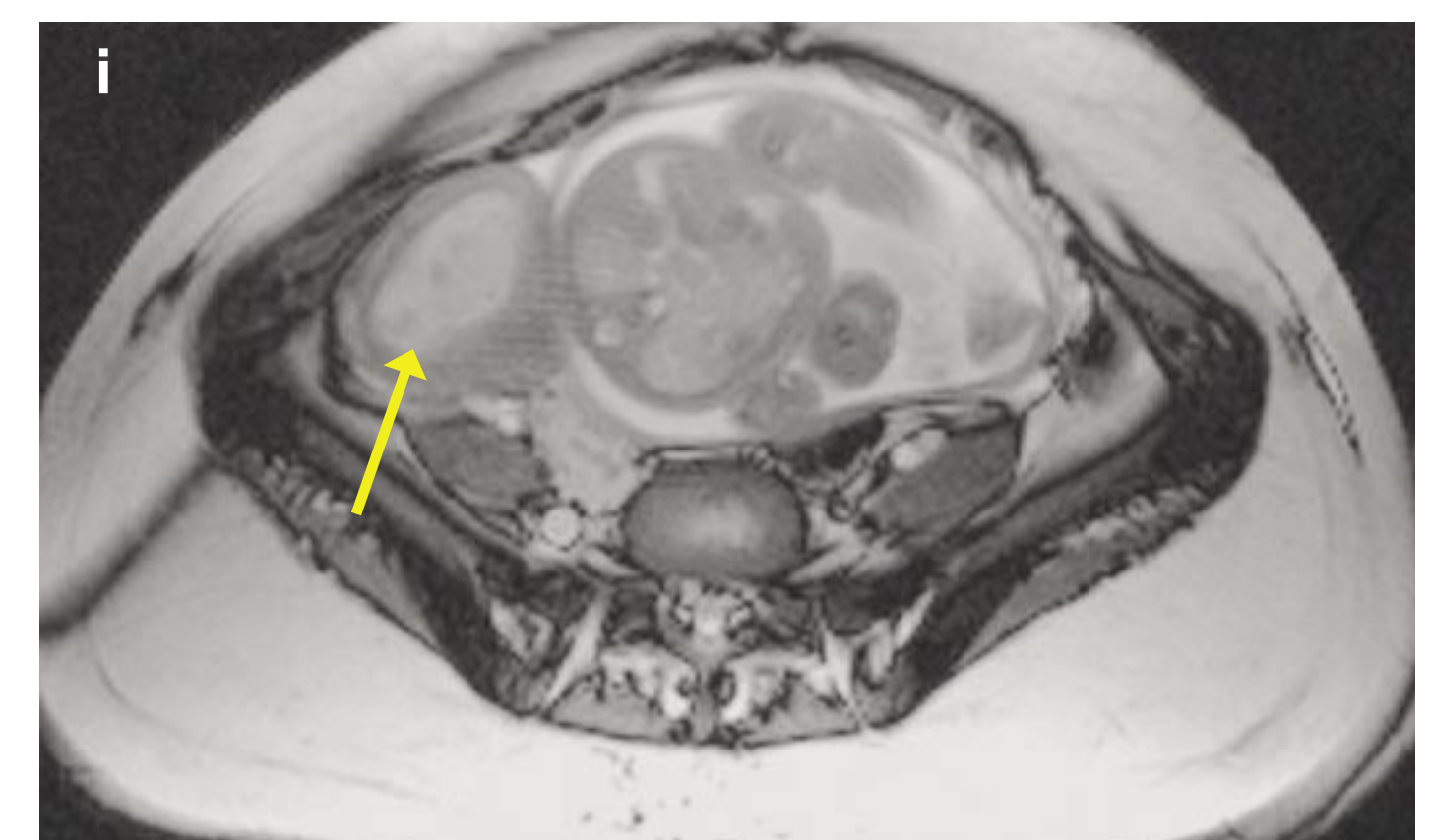
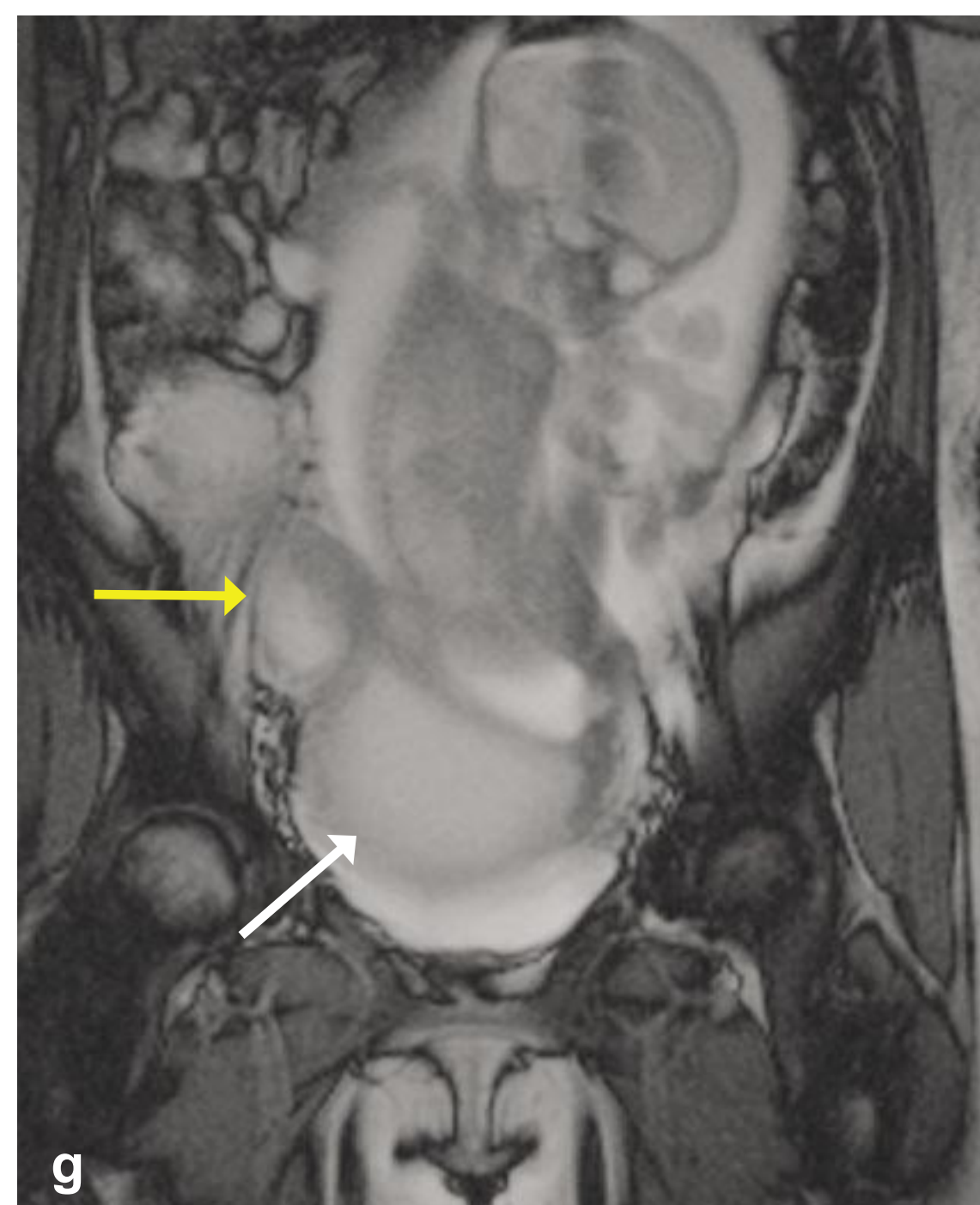
There does not appear to be impairment in fertility in patients with uterus didelphys (2). Even though the ability to conceive does not appear diminished, the ability to successfully complete the pregnancy to term is associated with many problems (3). Didelphic pregnancies are considered high risk (4) due to high miscarriage rate, premature rupture of membranes, cervical incompetence with premature labor, fetal malpresentation, increased risk of Cesarean section, and increased ante- and postpartum hemorrhage (3). This patient developed pre-eclampsia at 30 weeks unresponsive to medical treatment and underwent Cesarean section with low transverse incision. The right uterus measured approximately twelve weeks in size and contained organized clot. No surgical intervention to this uterus was performed but a septum was removed from the vagina.

In addition to reproductive problems, uterus didelphys is associated with renal and urinary tract anomalies given their common embryologic origins. At six weeks gestational age the mullerian and metanephric systems arise from a common ureteric bud (4). 75% of women with uterus didelphys demonstrate a transverse hemivaginal septum creating a double vagina, often with one side ending in a blind vaginal pouch (1).

Interestingly enough, unilateral renal agenesis occurs more often on the same side as the obstructed hemivagina (1). Renal agenesis is reported to occur in 84.6% of patients with an obstructed MDA as compared to 13.6% of nonobstructed systems (1). Discovery of uterus didelphys should therefore prompt an evaluation for associated renal anomalies. As in this patient the right kidney was not visualized. The right side of the vagina also contained the transverse septum.

Most patients present at, or shortly after, menarche often secondary to complications associated with the transverse vaginal septum. These patients can develop hematometra and hematocolpos with painful menses (5). Copious foul secretions can occur if a partial communication occurs between the patent vagina and partially obstructed vagina. Endometriosis is also a risk due to reflux of contents into the abdominal cavity (5). Many patients present with symptoms of acute abdomen which can lead to unnecessary surgeries such as appendectomies, salpingectomies, total hysterectomies, and dilation and curettage procedures (4). These procedures carry the potential for significant morbidity and mortality as well as loss of reproductive ability.

Diagnostic procedures previously employed in the literature include pelvic and rectal examinations, ultrasonography, vaginocopy, and laparoscopy (4). The advent of MRI with its exquisite detail of uterine anatomy can greatly assist diagnosis of MDAs in a non-invasive manner as well as evaluate for associated renal anomalies- thus avoiding unnecessary surgeries with their inherent risks (2).



Figures 4f-j. Sagittal, coronal and axial T2-weighted gradient echo MRI images show the obstructed right uterine cavity (yellow arrow) to the right of the fetus in the left uterine cavity. Blood within the obstructed upper vagina (white arrow) mimicked a mass inferior to the presenting fetal rump. Note the presence only of the left kidney on the coronal image (red arrow).

References

- Li, Sanying; et al. Association of renal agenesis and mullerian duct anomalies. COMPUT ASSIST TOMOGR 2000; 24 (6): 829-834.
- Baker, Philip N., et al. Uterus didelphys demonstrated with echo-planar magnetic resonance imaging. AM J OBSTET GYNECOL 1994; 170 (3): 813-814.
- Marcus, Samuel MD., et al The obstetric outcome of in vitro fertilization and embryo transfer in women with congenital uterine malformations. AM J OBSTET GYNECOL 1996; 175 (1): 85-89.
- Rey-Alvarez, Susana MD, PHD. A snake with two heads? Pitfalls in diagnosis and management of uterus didelphys with obstructed hemivaginae. ARCH PEDIATR ADOLESC MED 1997; 151 (6): 631-632.
- Cinelli, Ettore, MD., et al. Resectoscopic treatment of uterine didelphys with unilateral imperforate vagina complicated by hematocolpos and hematometra: case report. FERTIL STERIL 1999; 72 (3): 553-555.



ULTRASOUND CASE OF THE DAY

• Eric D. Sale, MD • Michelle L. Rodgers, MD • Lana G. Glenn, R.D.M.S. • Teresita L. Angtuaco, MD •
Department of Radiology, University of Arkansas for Medical Sciences, Little Rock, Arkansas

History

CASE 5

19-year-old woman presents to the Emergency Room with pelvic pain and vaginal bleeding.



Figure 5a. Transabdominal longitudinal ultrasound.



Figure 5c. Endovaginal sagittal ultrasound.

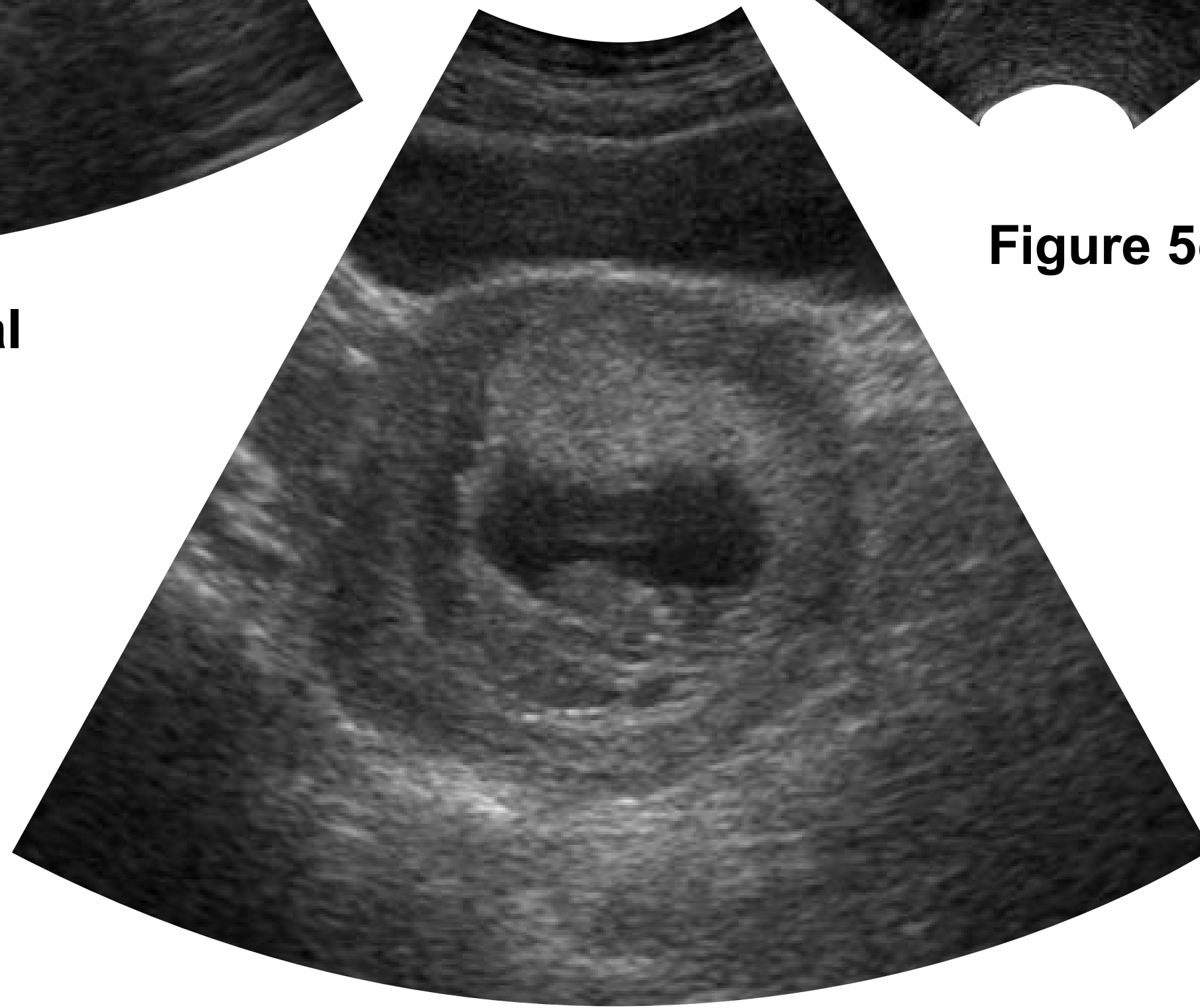


Figure 5b. Transabdominal transverse ultrasound.



Figure 5d. Endovaginal sagittal ultrasound.

Diagnosis

Subchorionic hemorrhage in an otherwise normal intrauterine pregnancy

Findings

The ultrasound demonstrates a single intrauterine pregnancy dating nine weeks by crown-rump length (Fig 5d). Beneath the chorion, a crescent-shaped hypoechoic rim is noted which represents subchorionic hemorrhage (Fig 5a, b and c). This large subchorionic hemorrhage is seen approximately 270 degrees around the gestational sac (Fig 5e and f). Normal cardiac activity was identified in the embryo in another plane. An anechoic cystic structure is visualized in the posterior aspect of the embryonic head corresponding to the open rhombencephalon (Fig 5c, d and g - yellow arrow). This is a normal finding. Another physiologic finding in this gestational age is separation of the amnion and chorion (Fig 5c, e and f).

Discussion

Normal embryologic development in the first trimester may mimic pathologic processes that occur in the second and third trimester (1). A few of these normal early gestational developments include chorioamniotic separation, open rhombencephalon, and physiologic anterior abdominal wall herniation. The amnion develops as an embryonic structure within and separate from the chorionic sac. The amnion grows throughout the first trimester and completely fills the chorionic cavity by the 15th or 16th week of gestation at which point the two membranes fuse. The primary separation before this time is a normal phenomenon. Amniocentesis prior to 16 weeks gestation is technically more difficult due to separation of the amnion and chorionic membranes (2).

Three primary brain vesicles develop during the 6th menstrual week: the prosencephalon, mesencephalon, and rhombencephalon. A small cystic structure seen in the posterior aspect

of the embryonic head represents the rhombencephalon which later develops into the fourth ventricle. This structure is routinely seen between the 8th and 12th menstrual weeks and should not be mistaken for a posterior fossa cyst (4).

Subchorionic hemorrhage is a common finding in the first trimester and may be associated with vaginal bleeding. This results from abruption of the edge of the chorion frondosum-decidua basalis complex or to marginal sinus rupture. (5) The chorionic membrane is stripped from the endometrium and elevated by the hematoma. Acute hemorrhage may be hyper-echoic or isoechoic relative to the placenta, and it becomes isoechoic in 1 to 2 weeks (1). In a group of patients presenting with vaginal bleeding between 10 and 20 weeks of menstrual age, identification of a subchorionic hemorrhage was associated with a 50% fetal loss rate. The prognosis appears to improve with a smaller volume of hematoma. (6)

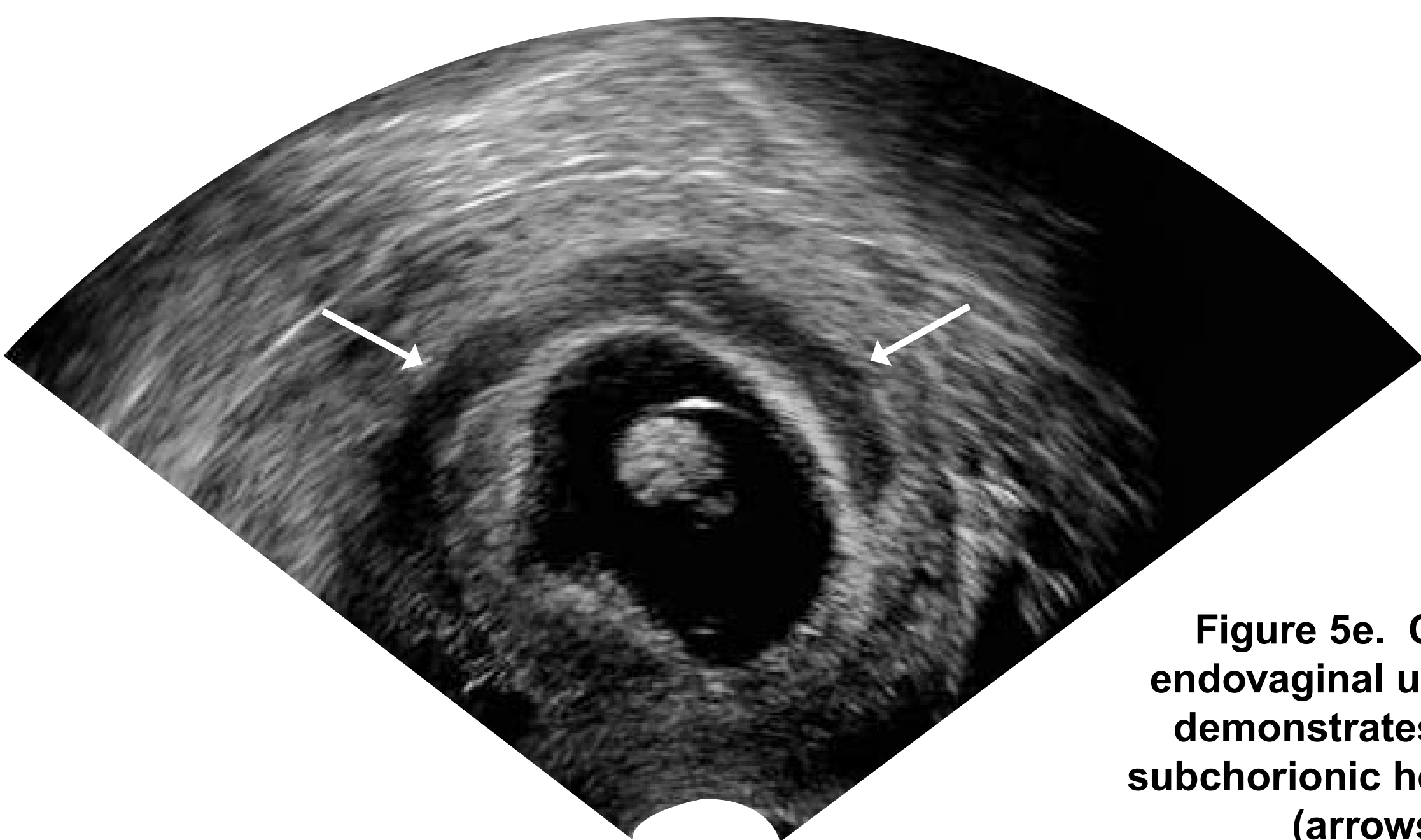


Figure 5e. Coronal endovaginal ultrasound demonstrates a large subchorionic hemorrhage (arrows).

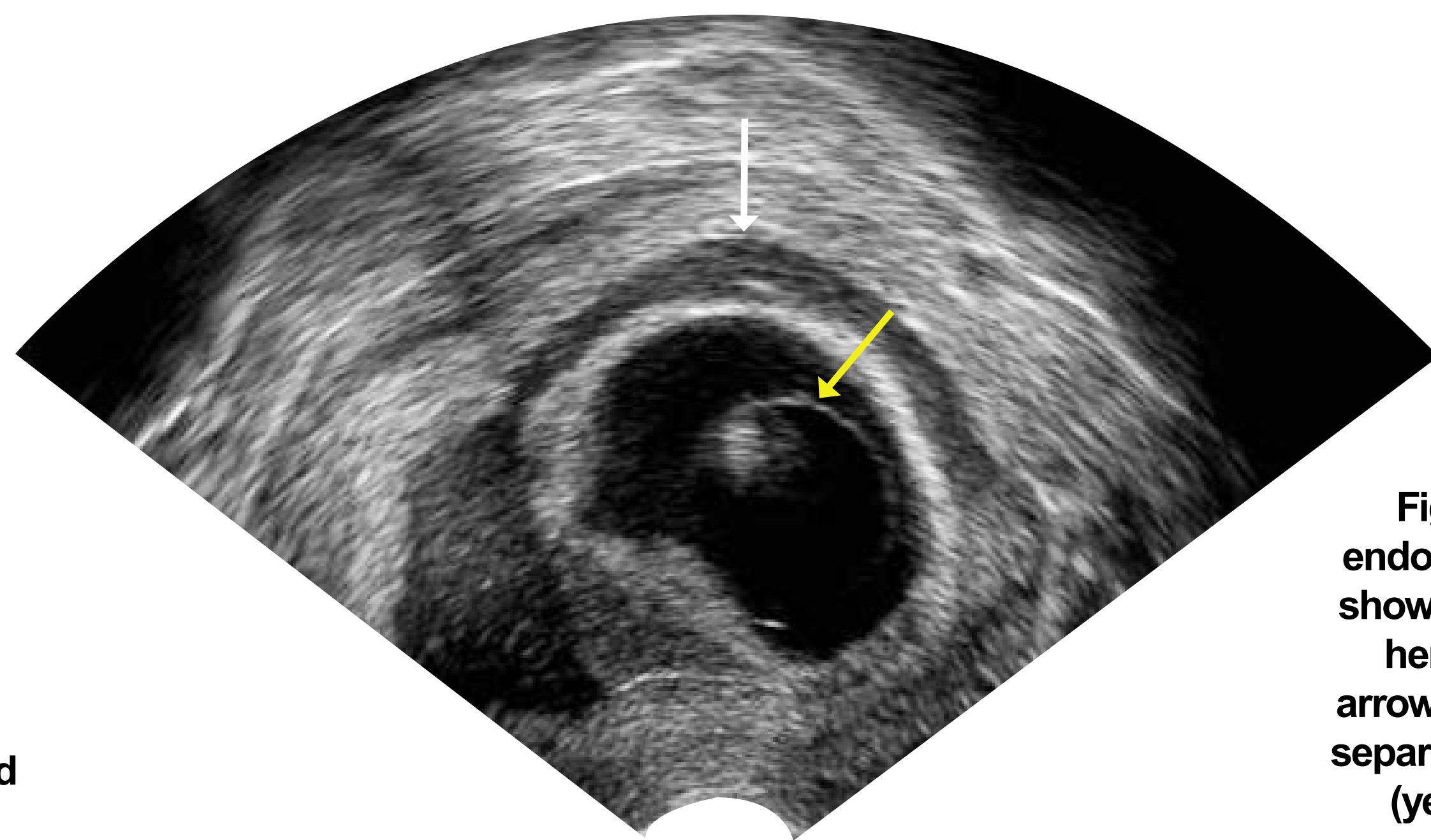


Figure 5f. Coronal endovaginal ultrasound shows the subchorionic hemorrhage (white arrow) as well as normal separation of the amnion (yellow arrow) and chorion.

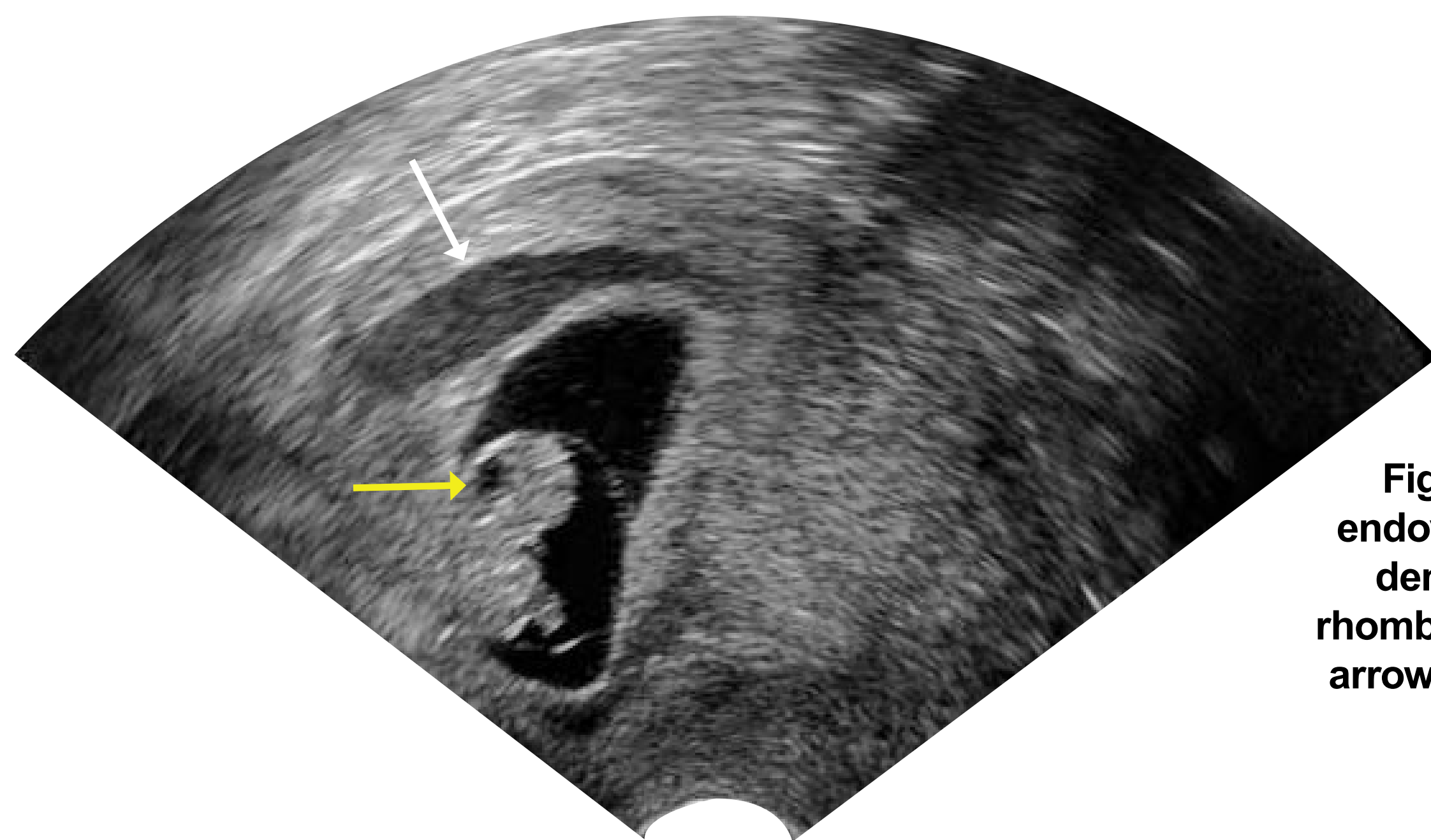


Figure 5g. Sagittal endovaginal ultrasound demonstrates open rhombencephalon (yellow arrow) and subchorionic hemorrhage (white arrow).

References

1. Rumack CM, Wilson SR, Charboneau JW. The First trimester. In: Diagnostic Ultrasound. Vol 2. St. Louis: Mosby-Year Book, Inc., 1991; 692-717.
2. McGahan JP, Goldberg BB. First trimester ultrasound. In: Diagnostic Ultrasound. A Logical Approach. Philadelphia: Lippincott-Raven Publishers, 1998; 143-150.
3. Cyr DR, Mack LA, Nyberg DA, et al. Fetal rhombencephalon: normal US findings. Radiology 1998;166:691-692.
4. Schmidt W, Yarkoni S, Crelin ES, et al. Sonographic visualization of physiologic anterior abdominal wall hernia in the first trimester. Obstetrics and Gynecology 1987;69:911-915.
5. Nyberg DA, Cyr DR, Mack LA, et al. Sonographic spectrum of placental abruption. AJR 1987;148:161.
6. Stabile I, Campbell S, Grudzinskas JG. Threatened miscarriage and intrauterine hematomas: sonographic and biochemical studies. J Ultrasound Med, 1989;8:289.